DEVELOPMENT OF A MODIFIED LINK BUDGET FORLOW EARTH ORBITING (LEO)-BASED LAND MOBILE SATELLITE COMMUNICATIONS SYSTEM

BY

MOSUNMOLA BOSEDESIDIKU

DEPARTMENT OFELECTRICAL AND COMPUTER ENGINEERING

FACULTY OF ENGINEERING

AHMADU BELLO UNIVERSITY,

ZARIA, NIGERIA

NOVEMBER, 2016.

DEVELOPMENT OF A MODIFIED LINK BUDGET FORLOW EARTH ORBITING (LEO)-BASED LAND MOBILE SATELLITE COMMUNICATIONS SYSTEM

BY

Mosunmola Bosede SIDIKU

B. Eng. (FUT MINNA) 2000

(P14EGEE8062)

smosunmola@gmail.com

A DISSERTATION SUBMITTED TO THE SCHOOL OF POSTGRADUATE STUDIES, AHMADU BELLO UNIVERSITY, ZARIA IN PARTIAL FULFILLMENT OF THE REQUIREMENTS FOR THE AWARD OF MASTER OF SCIENCE (M.Sc.) DEGREE IN TELECOMMUNICATION ENGINEERING.

DEPARTMENT OFELECTRICAL AND COMPUTER ENGINEERING

FACULTY OF ENGINEERING

AHMADU BELLO UNIVERSITY,

ZARIA, NIGERIA.

MAY, 2016

DECLARATION

I, Mosunmola BosedeSidikudeclare that the material in this dissertation entitled "Development of a Modified Link Budget for Low Earth Orbiting (LEO)-Based Land Mobile Satellite Communications System" and submitted for assessment on the programme of study leading to the award of Master of Science (M.Sc.)is entirely my own work and carried out by me in the Department of Electrical and Computer Engineering, Ahmadu Bello University, Zaria. The information taken from the work of others has been duly acknowledged in the text and a list of references provided. No part of this dissertation was previously presented for another certificate at this or any other Institution.

Sidiku Mosunmola Bosede _____ _____

Signature Date

CERTIFICATION

This Dissertation report titled the "Development of a Modified Link Budget for Low Earth Orbiting (LEO)-Based Land Mobile Satellite Communications System" by **Mosunmola Bosede SIDIKU** meets the regulations governing the award of the degree of Master of Science in Telecommunication Engineering of Ahmadu Bello University, and is approved for its contribution to knowledge and literary presentation.

Chairman Supervisory Committee	Signature	Date
(Dr S.M. Sani)	_____	_____
Member Supervisory Committee	Signature	Date
(Prof.M.B. Mu'azu)	_____	_____
Head of Department	Signature	Date
(Dr Y. Jibril)	_____	_____
Dean Postgraduate School	Signature	Date
(Prof. S.Z. Abubakar)	_____	_____

DEDICATION

I dedicate this work to my late father and mother; Barrister Disu Sidiku and Mrs Victoria Sidiku. May their gentle souls continue to rest in peace, Amen.

AKNOWLEDGEMENT

I am grateful to the Almighty God for making it possible for me to complete this research work. To him alone be the Glory, Honour and Power. I wish to express my deepest gratitude to everyone who has motivated me and /or supported me for the completion of this research work especially to my able supervisor Dr S.M Sani for his precious time, patient, constant support, constructive criticisms and immense contribution to this work. I say thank you for every seconds, minutes, days, months that you spent in going through my manuscript. I would also like to thank Professor M.B Mu'azu for his time, guidance, expert advice and immense contributions towards making this work a success.I also would like to extend my thanks to Prof. Bajoga, Dr. J. Yusuf, Dr. K. Abubilal, Dr. D. Usman, Dr. T. H. Sikiru, Dr. A. M. S. Tekanyi, Prof. B. Jimoh and Engineer Abdullahi Mohammedand his family (you are a friend indeed).Thank you all for your contributions and support. I would also like to thank all the staff of Electrical and Computer Engineering of ABU, for their assistance. I am also grateful to my senior colleagues in Engineering and Space Science; Advanced Computation Expert System Research Laboratory for their supports, especially Dr. O. A. Agboola, Dr. Ale Felix, Prof. B. Rabiu, Dr Mangete, Dr John Momoh, Dr Deji Inumoh, Yemson Rose, Olaniyi Bisola.This page will be incomplete without mentioning members of my family for their financial and moral support during the period; my best friend and husband, Olumotanmi Babajide Olanrewaju,sweet children Kadmiel and Tehila, my parents, Late Barrister Sidiku and Mrs Victoria Sidiku, my brothers and sisters and everyone that have contributed to my success in this programme. I thank you all for making my world a better place.

ABSTRACT

This research work presents the development of a Modified Link Budget for Low Earth Orbiting (LEO)-Based Land Mobile Satellite Communications System operating at Ku, K and Ka frequency bands by taking into cognizance the effect of additional loss due to Doppler frequency shift. Doppler frequency shift poses the problem of receiving higher or lower frequencies than the original transmitted frequency, this may be as a result of a relative movement between the source of the signal and the object (satellite or receiver) or both. In satellite communication system, this phenomenon constitutes the problem of signal loss.Effect of Doppler shift on satellite link budget is assumed negligible in conventional approach thereby resulting in the design of an unrealistic link budget, particularly in Low earth orbit (LEO) where it is more pronounced. In view of this, a more reliable approach to the estimation of satellite link budget at Ku, K, and Ka bands by the inclusion of Doppler frequency shift effect was investigated and its effect was investigated at different satellite orbits (LEO, MEO and GEO). The results obtained show that at maximum satellite converge angle and central frequencies for Ku, K and Ka bands, the Doppler frequencies for LEO (780 km) are: 325.50 kHz, 423.20 kHz and 726.90 kHz; for MEO (20000 km) we have 88.33 kHz, 114.80 kHz and 197.30 kHz; while GEO (35786 km) stood at 55.26 kHz, 71.84 kHz and 123.40 kHz . Variation of Doppler frequency shift with respect to the latitude (location) of the earth's terminal relative to the satellite motion was also studied. A typical earth terminal location in the range of 0 km – 100 km was selected for the study; from which it was verified that effect of Doppler shift in LEO increased as the distance from the initial location of the user terminal increased. These analyses further confirm that Doppler effect is more pronounced in LEO than in MEO and GEO. Comparative analyses between the conventional and the modified link

budget at Ku, K and Ka bands was achieved thereof. The results obtained show the Carrier to Noise density ratio for Ku frequency banddropped by 40% (from 25dB without Doppler shift to 15dB with Doppler shift). The Carrier to Noise density ratio for K frequency band dropped by 57% (from 70dB without Doppler shift to 30dB with Doppler shift). The Carrier to Noise density ratio for Ka frequency band dropped by 52% (from 110dB without Doppler shift to 53dB with Doppler shift).

This further confirmed that Doppler shift is most pronounced at LEO orbit hence the need to incorporate its effect in link budgeting. This work was validated against the work of Snehasis and Barsha, (2014).The results obtained through comparison show the Carrier to Noise density ratio for Ku frequency banddropped by 58% (from 31dB without Doppler shift to 13dB with Doppler shift). The Carrier to Noise density ratio for K frequency band dropped by 62% (from 54dB without Doppler shift to 20dB with Doppler shift). The Carrier to Noise density ratio for Ka frequency band dropped by 55% (from 85dB without Doppler shift to 38dB with Doppler shift). This clearly shows the need for inclusion of Doppler shift effect in LEO-based link budget.

TABLE OF CONTENTS

COVER PAGE i

TITLE PAGE ii

DECLARATION iii

CERTIFICATION.....iv

DEDICATION v

AKNOWLEDGEMENT vi

ABSTRACT vii

TABLE OF CONTENTS.....viii

LIST OF FIGURES..... xiii

LIST OF TABLES xiv

LIST OF ABBREVIATIONS xv

CHAPTER ONE: INTRODUCTION

1.1 Background..... 1

1.2 Aim and objectives..... 4

1.3 Statement of problem..... 5

1.4 Methodology 5

1.5 Significant contribution of the Research 6

1.6 Thesis outline..... 8

CHAPTER TWO: LITERATURE REVIEW AND THEORETICAL BACKGROUND

2.1 Introduction..... 9

2.2 Review of fundamental concepts..... 9

2.2.1 Atmospheric Absorption loss 10

2.2.2 Attenuation caused by rain..... 10

2.2.3 Attenuation caused by cloud or fog..... 11

2.2.4 Attenuation caused by snow 11

2.2.5 Scintillation of atmospheric and Ionospheres..... 12

2.2.6 Gaseous Absorption..... 12

2.2.7 Polarization loss or polarization effects..... 13

2.2.8 Free Space loss..... 13

2.2.9 Antenna Misalignment Loss 14

2.2.10 Feeder Line Loss 15

2.2.11 Total transmission path loss..... 15

2.2.12 Doppler frequency Shift..... 16

2.2.13 Classical Link Budget analysis..... 19

2.3.13.1Effective Isotropic Radiated power.....19

2.3.13.2 Power Flux Density.....19

2.3.13.3 Antenna gain.....20

2.3.13.4 Link Power equation.....21

2.3.13.5 Figure of Merit.....22

2.3.13.6Carrier of Noise Density Ratio.....23

2.3.13.7 Energy per bit to noise density.....23

2.3.13.8 Overall conventional Link Budget.....24

2.3.13.9Link Margin..... 25

2.2.13.10 Radio Frequency Band..... 25

2.2.13.10.1 L band 26

2.2.13.10.2 S band.....26

2.2.13.10.3 C band 26

2.2.13.10.4 X band.....27

2.2.13.10.5 Ku band.....27

2.2.13.10.6 Ka band.....27

2.2.13.11 Modulation.....27

2.3 Review of Similar Research Work.....29

CHAPTER THREE: DESIGN METHODOLOGY

3.1 Introduction 34

3.2 Methodology..... 34

3.2.1Selection of Key Parameters.....34

3.2.1.1 Selection of carrier frequency.....35

3.2.1.2 Selection of satellite transmit power.....36

3.2.1.3 Selection of modulation and demodulation 37

3.2.2Development of a Mathematical Model of Doppler Frequency shift.....37

3.2.2.1 Effect of the earth's Terminal Location on Doppler Frequency.....41

3.2.3 Development of a Modified Model of Satellite Link Budget by including Doppler Effect.....42

3.3 Modified Link Model Validation 44

3.4 Conclusion.....46

CHAPTER FOUR:RESULTS AND ANALYSIS

4.1 Introduction.....47

4.2 Variation of Doppler Frequency with orbital height 47

4.3 Effect of user terminal Location on Doppler frequency.....49

4.4 Variation of carrier to noise density ration with transmission path loss.....50

4.4.1 Variation of carrier to noise density ratio with transmission path loss at Ku band... 51

4.4.2 Variation of carrier to noise density Ratio with transmission path loss at K band....52

4.4.3 Variation of carrier to noise density ratio with transmission path loss at Ka band... 53

4.5 Modified Link Budget Validation Results.....53

4.6 Conclusion.....56

CHAPTER FIVE:CONCLUSION AND RECOMMENDATION

5.1 Introduction.....58

5.2 Conclusion 58

5.3 Recommendations for Further Work.....59

References.....60

Appendix.....64

LIST OF FIGURES

Figure 1.1..... 2

Figure 2.1..... 14

Figure 2.2..... 17

Figure 3.1..... 37

Figure 3.2..... 41

Figure 4.1..... 47

Figure 4.2..... 49

Figure 4.3..... 50

Figure 4.4..... 51

Figure 4.5..... 52

Figure 4.6..... 53

Figure 4.7..... 54

Figure 4.8..... 55

Figure 4.9..... 56

LIST OF TABLES

Table 1.1..... 3

Table 2.1..... 26

Table 3.1..... 35

Table 3.2..... 36

Table 3.3..... 45

Table 4.1..... 48

LIST OF SYMBOLS

Acronyms	Definition
LEO	Low Earth Orbiting
MEO	Medium Earth Orbit
GEO	Geostationary Orbit
C / N_0	Carrier to Noise Density Ratio
GEOS	Geostationary Satellite
$\left(E_b / N_0\right)$	Energy per bit Noise Density Ratio
HPBW	Half Power Beam Width
TFL	Transmission Feeder Loss
TPL	Total Path Loss
AML	Antenna Misalignment Loss
FSL	Free Space Loss
AAL	Atmospheric Absorption Loss,
GAL	Gaseous Absorption Loss
EIRP	Effective Isotropic Radiated Power
$G(\theta)$	Gain of an Antennae at angle

G/T	Figure of Merit
$\frac{P_{ri}}{N_O}$	carrier power to noise density
FEC	Forward Error Correction
LM	Link Margin
RF	Radio Frequency
GPS	Global Positioning System
TV	Television
FM	Frequency Modulation
FSK	Frequency Shift Key
M-ary PSK	M-ary Phase Shift Keying
QPSK	Quadrature Phase Shift Keying
BPSK	Binary Phase Shift Keying
BER	Bit Error Rate
SAF	Store-And-Forward
HPA	The High Power Amplifier
EIRP	Equivalent Isotropic Radiated Power
KPA	Klystron Power Amplifier

SSPA	Solid State Power Amplifier
TWTA	Traveling Wave Tube Amplifier
$\vec{V}_{rel}$	Satellite Velocity

CHAPTER ONE

INTRODUCTION

1.1 BACKGROUND

In recent years, low earth orbit (LEO) satellites have been employed to carry signals for large population of simultaneous users in mobile satellite communication systems over communication link. LEO satellites have very wide scientific applications such as but not limited to; remote sensing of oceans, analyses of Earth's climate change, Earth's imagery with high resolution and astronomical purposes. Low earth orbit satellites are also used for data relay and navigation as well as low-cost store-and-forward communications systems. This technology is currently being used for communicating with mobile terminals and with personal terminals that need stronger signals to function. Examples of satellite networks in this orbit include Iridium system with sixty six (66) satellites and Globalstar system's forty eight (48) satellites (Ray, 2000).

The low earth orbit is located at a height range of 106 - 2000km above the earth surface (Qingchong, 1999) as shown in Figure 1.1. The speed of LEO satellites is high, with a very negligible round trip delay of about 10-20 ms and its orbital period is about 100 minutes(Raymond, 1996). Each LEO satellite is only visible from the earth for about 10 to 20 minutes. Communications between two earth stations typically will involve handing off the signal from one satellite to another. The low earth orbit have attracted the most attention because of technical advantages and the novelty of having many satellites, hand-offs and a cellular-like configuration (Jamalipour, 1997).

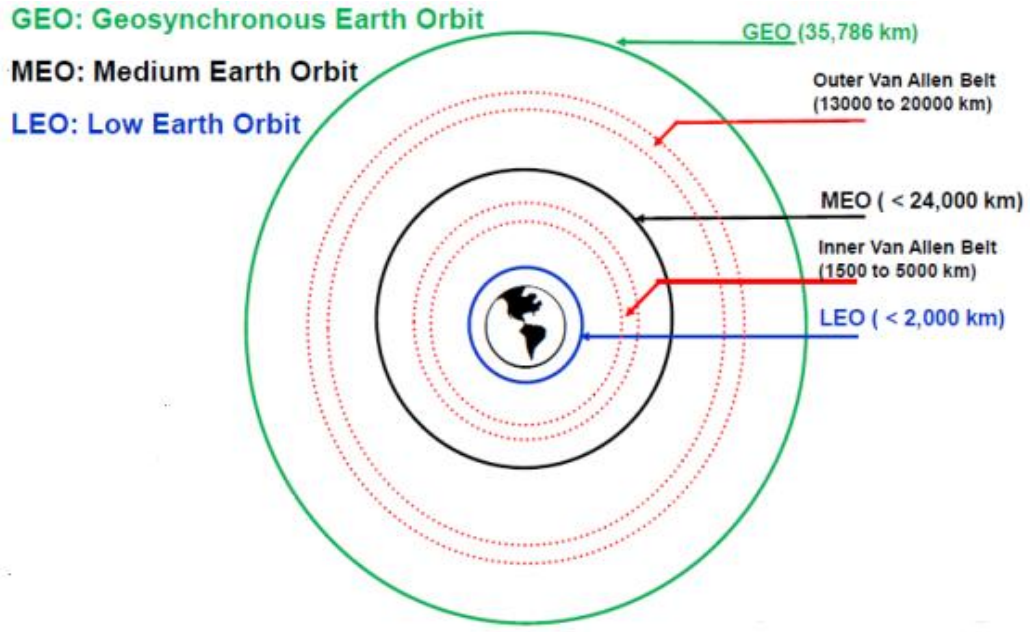


Figure 1.1: LEO, MEO and GEO Satellite Orbits (Adria, 2010)

The advantages of Low earth Orbit (LEO) include small propagation loss which allows mobile users to use handsets for direct communication, and a small propagation delay (about 10ms compared to 250ms for Geostationary satellite (GEOS)) for better voice performance, and other interactive services. The technical characteristics of satellite orbits are shown in Table 1.1. In addition, Low Earth Orbiting (LEO) Satellites do not suffer from consistent low elevation angles at high altitudes and the associated propagation that Geostationary (GEO) satellites do rather, with proper inclinations, LEO can cover high latitude locations, including polar areas, which cannot be reached by GEO satellites (Raymond, 1996).

Table 1.1: Technical Characteristics of Satellite Orbits (Ogundele, 2010)

S/N	Low Earth Orbit (LEO)	Medium Earth Orbit (MEO)	Geostationary orbit (GEO)
1	Altitude: less than 2000 km above the Earth's surface in a circular orbit.	Altitude: Located 8,000 to 24,000 km (5k to 15k miles) above the Earth's surface in circular orbit.	Altitude: Located 35,786 km (22,236 miles) above the Earth's equator in a circular orbit
2	Most LEO constellations have a circular orbit, which is inclined from the equator, up to polarorbit (90° inclination). Multiple inclinations used.	Most MEO constellations are inclined from the equator, up to polar orbit (90° inclination). Multiple inclination planes are often used.	
3	Orbital velocity: ~28,080 km/hr (17,448 miles/hr).	Orbital velocity: ~18,000 km/hr (11,184 miles/hr).	Orbital velocity: 11,066 km/hr (6,876 miles/hour).
	One orbital period: 90 minutes to 3 hours	One orbit: 6 to 14 hours, depending on altitude.	One orbit: 23hr 56min 4sec (= Earth's rotation).

4	Angular separation: 30° to 60°, depending on number of LEOs in each inclined plane		Angular separation: ~ 2° (1,476 km; 920 miles).
5	Visible time with Earth Station: 10 to 20 minutes	Visible time with Earth Station: 75 to 8 hours depending on latitude	Visible time with Earth Station: 24 hours.
6	Service life expectancy: 5 to 8 years	Service life expectancy: Longer then LEOs, but less then GEO satellites.	Service life expectancy: 15 yrs or more.

The major disadvantages of the LEO orbit are; more satellites are required, there is increased probability of atmospheric drag, phase error and Doppler frequency shift.

The Doppler frequency shift poses the problem of receiving higher or lower frequencies than the original transmitted frequency. It is defined as the rate of change in signal phase over time relative to the receiver (Jamalipour, 1997). The concept of Doppler frequency shift is applicable to the land mobile radio, including digital cellular transmission link. Here, the cause of Doppler effect could be due to the movement of a mobile unit or natural and constructed obstacles. Natural calamities like torrential rains, raging storms, heavy snowfall e.t.c also cause significant Doppler effect in wireless communication (Kausik et. al, 2007).

In a LEO satellite system, Doppler shift can be introduced in the both uplink and downlink reasons being that if not accounted for during link budget, this Doppler effect can cause serious degradation of demodulation performance and frequent failure of radio link. (Jamalipour, 1997).

1.2 MOTIVATION OF RESEARCH

Effect of Doppler shift on satellite link budget is assumed negligible in conventional approach thereby resulting in the design of an unrealistic link budget, particularly in Low earth orbit (LEO) where it is more pronounced. The prime motivation of this research work is to give an insight on the effect of Doppler on satellite link budget in LEOby first elucidating its adverse nature and then accounting for the losses thereof via a better link design.

1.3 SIGNIFICANCE OF RESEARCH

Doppler shift is defined as the change in frequencies of a wave (signal) as a result of a relative movement between the source of the signal and the object (satellite or receiver). In satellite communication system, this phenomenon constitutes the problem of signal loss.Conventional Satellite Link budget design which is a key ingredient for effective communication between the satellite and the earth terminal did not take into consideration the effect of Doppler shift particularly in Low earth orbit (LEO) where it is more pronounced.In view of this, a more reliable approach to the estimation of

satellite link budget at Ku, K, and Ka bands by the inclusion of Doppler frequency shift effect was investigated and the effect of Doppler shift with respect to the position of the orbiting satellite and earth's terminal was also critically examined.

1.4 STATEMENT OF PROBLEM

The determination of the satellite link budget is made very complex by orbit perturbations which the satellite experiences as it travels along its track. These perturbations include atmospheric drag and Doppler frequency shift. If these problems are not accounted for during link budget, they can cause serious degradation of the signal propagating on the transmission link which may eventually lead to the link failure. Despite the extensive work done in the prediction and analysis of mobile satellite link, the links are still unreliable due to shift in frequencies caused by motion of transmitter receiver or both, particularly in the Low Earth Orbit where Doppler effect is significant.

The conventional approach used in the link budget analysis as described in the literatures reported herein was not representative enough to achieve a robust communication link design for LEO because of the omission of signal impairment due to Doppler frequency shift.

Furthermore, to the best of my knowledge, there has not been a scientific justification as to why the Doppler effect was not considered or included in link budgeting especially, for satellite in LEO orbit. This research work therefore presents an improved LEO-based link budget for land mobile satellite communication by taking into account losses due to Doppler frequency shift on both uplink and downlink paths by considering its effect on the range of earth's terminal and on carrier to noise density ratio.

1.5 AIM AND OBJECTIVES

This research is aimed atdeveloping a Modified Link Budget for Low Earth Orbiting (LEO)-Based Land Mobile Satellite Communications System operating at Ku, K and Ka frequency bands by considering the effects of Doppler frequency shift centered on the following objectives:

i. To develop a more reliable analytical approach to the estimation of satellite link budget by inclusion of Doppler frequency shift in the conventional link budget model.
ii. To carry out quantitative analysis of the effect of Doppler frequencyshift at higher microwave frequency bands (Ku, K and Ka bands) in LEO, MEO and GEO with focus on its severity and the effect of earth’s terminal location on the Doppler frequency shift in relation to the position of satellite in LEO.
iii. Need to validate the results

1.6 METHODOLOGY

i. Selection of carrier frequency, satellite transmitter power and methods of modulation and demodulation.

ii. Development of a mathematical model of Doppler frequency shift.

iii. Development of a modified model of a satellite link budget by including Doppler effect.

iv. Simulation of the modified link budget at Ku, K and Ka bands using MATLAB R 2014a version.

v. Comparison between the simulated results obtained for both modified and conventional link budgets at Ku, K and Ka bands.

vi. Validation using comparative analysis

1.7 DISSERTATION ORGANIZATION

The general introduction has been presented in chapter one.The rest of the research work is organized as follows; Fundamental concepts pertinent to the design of a satellite link budget in the Low Earth Orbit (LEO) and a critical review of published similar research works is provided in the next chapter.Chapter three presents the procedures as well as an in-depth analysis leading to a more reliable approach to satellite link budget estimation. Comparison between the link budget modeled with Doppler effect and the conventional link budget analysis without the Doppler effect is also made in this chapter. Chapter four focuses on the interpretation of the results based on the analyses presented in the chapter three. Chapter five contains conclusions, significant contributions, limitations and recommendations for future work. Quoted references and appendices are provided at the end of the dissertation report.

CHAPTER TWO

LITERATURE REVIEW AND THEORETICAL BACKGROUND

2.1 INTRODUCTION

The literature review comprises of the review of fundamental concepts pertinent to the design of a satellite link budget in the Low Earth Orbit (LEO) and a critical review of published similar research works.

2.2 REVIEW OF FUNDAMENTAL CONCEPTS

Satellite link design involves a mathematical approach to the selection of link subsystem variables in such a way that the overall system performance criteria are met. The most important performance criterion is the signal quality; that is, the energy per bit noise density ratio $\left(E_b/N_0\right)$ in the information channel, which carries the signal in the form which is delivered to the user(s) (Ogundele, 2010). This electrical signal contains data or information with different voltage level which represents the data information streams. If the transmission medium is perfect then the receiver will get the exact signal which was send by the transmitter during transmission. However, communication means are generally not 100% efficient; therefore, the received signal will not be exact replica of its transmitted version (Ogundele, 2010). The impairment of signals leads to errors in signal information. Communication link suffers from different problems and they constitute what is known as link losses, (Ray, 2000):

i. Atmospheric Absorption Loss
ii. Attenuation caused by rain (absorption and scattering)
iii. Attenuation caused by cloud or fog
iv. Attenuation caused by snow
v. Gaseous Absorption
vi. Tropospheric scintillation

vii. Polarization effect

viii. Free space loss

ix. Antenna Misalignment Loss

x. Feeder Line Loss

xi. Doppler frequency shift

2.21 Link Losses

link loss encountered on satellite communication link are described briefly below.

2.2.2 Atmospheric Absorption Loss

These are losses mainly due to oxygen, water vapour and rainfallin the air (William, 1999).It is very low in the range 0.3 - 1dB (Lower than 1dB) and decreases as the elevation angle increases.

2.2.3 Rain Attenuation

This attenuation is caused by the scattering and absorption of electromagnetic waves by drops of liquid water. The scattering diffuses the signal, while absorption involves the resonance of the waves with individual molecules of water. Absorption increases the molecular energy, corresponding to a slight increase in temperature, and results in an equivalent loss of signal energy.Rain affects the transmission of an electromagnetic signal by attenuating the signal; increasing the system noise temperature; and changing its polarization. All three of these mechanisms cause degradation in the received signal quality and become increasingly significant as the carrier frequency increases (Ray, 2000).

The attenuation and is expressed as (William, 1999):

$$\gamma = KR^{\alpha} \qquad (2.1)$$

Parameter K and α are constants and depend on frequency, raindrop size distribution, rain temperature and polarization. R is the rain rate.

2.2.4 Attenuation caused by Cloud or Fog

Clouds and fog can produce many losses for low elevation angles at high frequencies(William, 1999). As the elevation angles increases, their effect becomes less significant. Similarly, even for low elevation angles, their effect can be neglected at frequencies below 5GHz(William et al, 1999);The attenuation caused by Fog is expressed as:

$$L_f = \frac{0.148 f^2}{\vartheta_m^{1.43}} \text{ (dB/km) (Always less than 0.03dB)} \quad (2.2)$$

Where:*f* = frequency GHz

ϑ_m=(m) is the visibility,Heavy fog:$\vartheta_m < 50m$,

Median fog: $50 \leq \vartheta_m < 200m$, Light fog: $50 \leq \vartheta_m < 500m$

2.2.5Attenuation caused by Snow

Snow may have some fading effect on reflector antennas, specially, when the reflector is looking vertically. Dielectric losses of dry snow can be neglected. However, asymmetrically gathered snow can distort the antenna's beam causing phase delay that can theoretically lead to the complete disappearance of the signal in extreme cases(Adria, 2010). Nevertheless, this effect can be easily prevented if accumulated snow is removed from time to time from the reflector's surface (Adria, 2010);The attenuation caused by snow is expressed as:

$$L_s = 7.47 \times 10^{-5} \times I \ \ 1 + 5.77 \times 10^{-5} f^3 I^{0.6} \quad \text{(dB/km)} \quad (2.3)$$

Where: *f* = frequency GHz, *I*(mm/H) is the strength of snow.

2.2.6 Tropospheric Scintillation

Tropospheric scintillations are amplitude fluctuations produced by refractive inhomogenieties present in the lowerpart of the troposphere. Scintillation can occur with or without fading on the path; the former is known as dry scintillation and the latter as wet scintillation since it is accompanied by rain on the path. The magnitude of scintillation increases with the increase of frequency, decrease of elevation angle, and decrease of the antenna diameter (Asoka, 2002).

2.2.7 Gaseous Absorption

Compared to other absorptive effects, gaseous absorption, from oxygen and water vapor present in the atmosphere is relatively small. Absorption due to oxygen is nearly constant and that due to water vapor varies slowly with time in response to variations in the water vapor content in the atmosphere. As such, the gaseous absorption increases with the relative humidity as well as the temperature (Asoka, 2002).

2.2.8 Polarization Loss orPolarization Effects

Polarization loss occurs due to any polarization mismatch between the transmitting and receiving antennas. The polarization loss will be, in worst case, 3dB, when transmitting with linear polarization and receiving with circular polarization (William, 1999).Linear polarized system is prone to the effect

of polarization rotation when waves propagate through the earth's ionosphere in the presence of the earth's magnetic field. The effect of polarization can be prevented by using circular-polarized signal(William et al, 1999).

2.2.9 Free Space Loss

The free space path loss is caused by the reduction of flux density due to the distance the signal travels and the receiving ability to absorb the emitted energy (Dennis,2001). The free space path loss is determined by the maximum distance and the frequency of the radio signal. For satellite communication this is the primary mode of signal loss. Free space loss is the most significant loss of the propagation losses, and it depends on frequency and on the distance between the satellite and the ground station. It is calculated in dB, using the following equation (Adria, 2010):

$$F_{sl} = 20\log\left(\frac{4\pi}{C}\right) + 20\log(R_s) + 20\log(f)dB \quad (2.4)$$

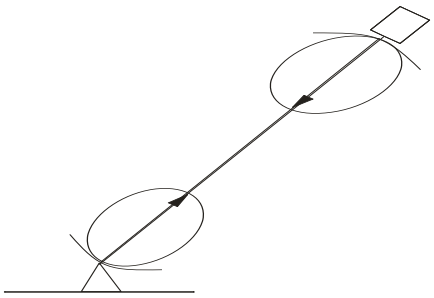
$$F_{sl} = -147.56 + 20\log(R_s) + 20\log(f)dB \quad (2.5)$$

Where:$R_s$is the range between the ground station and a satellite, f is the signal frequency and C is the speed of light.

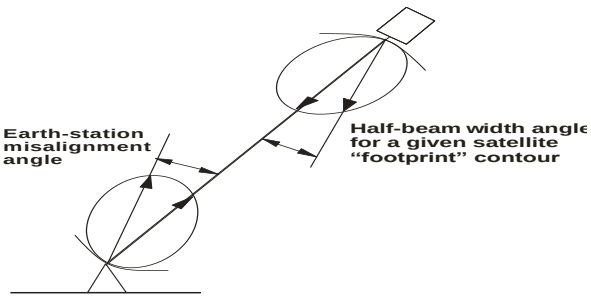
The actual distance between the satellite and the station depends on the elevation angle(Dennis,2001). It increases as the elevation angle decreases, hence causing an increase in the total losses. Moreover, the free space path losses are directly proportional to frequency. As a result, thehigher the frequency, the higher the losses.

2.2.10 Antenna Misalignment Loss

When a satellite link is established, the ideal situation is to have the earth and the satellite antennas aligned for maximum gain, as shown in Figure 2.1 (a). From this Figure, two possible sources of off axis loss are identified: one at the satellite and the other at the earth station.The off axis at the earth station is referred to as the antenna pointing losses which are usually only a few tenths of a decibel(Seybold, 2005).



(a)Satellite and Earth Station Antennas Aligned for Maximum Gain



(b) Earth Station Antennas Misaligned

F

Figure 2.1: Earth Station Situated on a Satellite Footprint(Dennis, 2001)

Causes of misalignment are the angle deviation of the rotator, the structure, and the reflector and feed themselves, as well as, misalignment in the satellite antenna(Seybold, 2005). Due to the misalignment, the actual gain will decrease, resulting in a pointing losses or antenna misalignment loss in dB(Maral, 2002) as show below:

$$AML = 12\left(\frac{Pointing\ error}{HPBW}\right)^2 \qquad (2.6)$$

but;

$$HPBW = \frac{21}{Df} \qquad (2.7)$$

where,

HPBW = Half Power Beam Width, *D* = diameterof the dish and *f* = signal frequency.

2.2.11 Feeder Line Loss

The feeder losses occur at the joint connecting the receiver antenna and the receiver proper; and the same is applied to the transmitter (NIIT, 2007).

Such losses occur in the connecting waveguides, filters and couplers.

2.2.12 Total Transmission Path Loss

The transmission path loss or tpl is the summation of all the losses and it is defined as (NIIT, 2007);

$$tpl = fsl + pl + aml + aal + Gal + Rl + fl + sl + tp \qquad (2.8)$$

Where: fsl = free space loss, *aml* = antenna misalignment loss, *pl*= polarization loss and *aal* = atmospheric absorption loss, Gal = gaseous absorption loss, Rl = rain attenuation, fl = attenuation caused by clouds and fog, sl = loss due to snow and

tp = tropospheric attenuation.

2.2.13 Doppler Frequency Shift

The reception of higher or lower signal frequencies than the original transmitted frequency is due to phenomenon known as Doppler frequency shift; and it is a practical problem in satellite communication (Levano, 1988). As the satellite moves, a Doppler shift of the downlink is produced as observed by the user terminal and a corresponding frequency shift of the uplink as perceived by the satellite (Gataullin et al., 2010).

Among different types of non-geostationary orbits, there exist two conventional orbits for the communication satellites: low-altitude and highly elliptical orbits(Naser et al., 2001). Notably, satellite in non-geostationary orbit changes its position relative to the Earth. As a result of this, signal experiences a Doppler shift whose value and drift rate are very significant as oppose to that obtained with satellite in geostationary orbit(Naser et al., 2001). In order to accurately calculate the Doppler frequency shift, a relative velocity between satellite and ground terminal is required. Figure 2.2 shows a typical representation of a satellite dynamics in orbit.

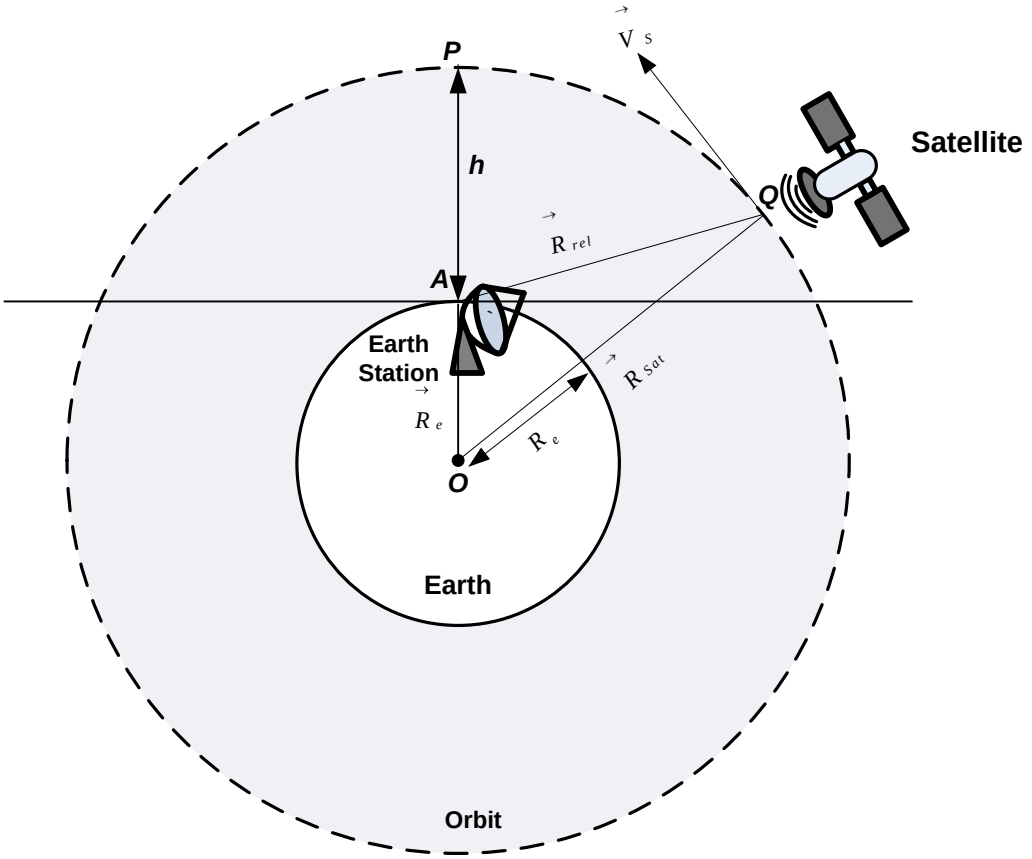


Figure 2.2: Typical Representation of Satellite Dynamics in an Orbit (Naser et al., 2001)

To compute the relative velocity of the Earth's terminal and the satellite, the ground station and the satellite velocity vectors must be in the same coordinate reference frame (Naser et al., 2001). If $\vec{R}_e$ and $\vec{R}_{Sat}$ are the position vectors of the user terminal or Earth's station terminal and satellite respectively, then relative position of the satellite and Earth's terminal is given by (You et al., 2000):

$$\vec{R}_{rel} = \vec{R}_{Sat} - \vec{R}_e \quad (2.9)$$

The relative velocity of the satellite and Earth's terminal is given by;

$$\vec{V}_{rel} = \frac{d\,\vec{R}_{rel}}{dt} = \frac{d\left(\vec{R}_{Sat} - \vec{R}_e\right)}{dt} \quad (2.10)$$

Equation (2.10) can further be expressed in terms of magnitude and direction by as;

$$\vec{V}_{rel} = \vec{V}_S \cdot \hat{\vec{R}}_{rel} \quad (2.11)$$

Where $\hat{\vec{R}}_{rel}$ is the position vector of $\vec{R}_{rel}$ given by;

$$\hat{\vec{R}}_{rel} = \frac{\vec{R}_{rel}}{\left|\vec{R}_{rel}\right|} \quad (2.12)$$

During Doppler effect, the received and transmitted signal frequencies are related by the following equation (Gataullin et al., 2010);

$$f_r = f_t \pm f_{ds} = f_t \pm \frac{\left|\vec{V}_{rel}\right| f_c}{C} \quad (2.13)$$

Where:

f_r and f_t are the received and transmitted signal frequencies respectively.

f_c is the carrier wave frequency.

f_{ds} is the Doppler shift frequency.

$\left|\vec{V}_{rel}\right|$ is the magnitude of the relative velocity between the satellite and the Earth's terminal.

C is the velocity of electromagnetic wave.

It can be deduced from equation (2.13) that the Doppler shift frequency is given by (Gataullin et al., 2010);

$$f_{ds} = \pm \frac{\left|\vec{V}_{rel}\right| f_c}{C} \quad (2.14)$$

The ambiguous sign in equation (2.14) explains the scenarios where the satellite is either ascending towards horizon or receding below it with respect to the position of the Earth's terminal.

2.2.14 Classical Link Budget Analysis

A link budget is simply the addition and subtraction of gains and losses in a radio link. When the gains and losses of various system components are summed together, the result is an estimation of the system performance in the real world (Maral, 2002). To arrive at an accurate answer, every component or factor that contributes to gain or loss must be included. Detailed reviews of these factors are provided in the following subsections:

2.2.14.1 Effective Isotropic Radiated Power

The Effective Isotropic Radiated PowerEIRP(dBW) is a key parameter in link budgetdenoted as EIRP. It is regarded as one of the parameters of meritfor the transmit portion of the link, and can be calculated in dBm (Pratt, 2003). EIRP describes the combination of a transmitter power and antenna gain in terms of an equivalent isotropic source with power P_t watts, radiating uniformly in all directions (Pratt, 2003). EIRP is expressed mathematically as (Pratt, 2003):

$$EIRP = P_t + G_t \quad (2.15)$$

Where:$[p_t]$ = transmitted power and $[G_t]$ = transmit antenna gain.

2.2.14.2 Power Flux Density

The power flux density, F, is an important parameter in the evaluation power requirements and interference levels for satellite communications networks(Pratt, 2003). This parameter refers to received power density on the surface located at a distance 'r' from the transmitting antenna. It is expressed in W/m^2: (Burdic,1984)

$$F = \frac{P_t G_t}{4\pi R^2} \quad (2.16)$$

Where: *F* = Flux Density, P_t = Transmitting RF power i.e. total power radiated by the transmitting source, *R* = Radius of the spherical surface and G_t = Transmitting antenna gain.

2.2.14.3 Antenna Gain

All real antennas are directional and radiate more power in some directions than in others. Any real antenna has a gain *G(θ)*,defined as the ratio of power per unit solid angle radiated in a direction θ to the average power radiated per unit solid angle: (Louis, 2008)

$$G(\theta) = \frac{P\ \theta}{P_0 / 4\pi} \quad (2.17)$$

Where:*P(θ)* = power radiated per unit solid angle by the antenna, P_0 = total power radiated by the antenna and *G(θ)* =gain of the antenna at an angle.

The reference for the angle ϑ is usually taken to be the direction in which maximum power is radiated, often called the bore sight direction of the antenna (Louis, 2008). The gain of the antenna is then the value of *G(θ)* at$\theta = 0^0$ angle, and is a measure of the ratio of increase in flux density radiated by the antenna to that from an ideal isotropic antenna radiating the same power (Louis, 2008). Isotropic power radiation is usually not effective for satellite communications links; because the power density levels will be low for most applications except mobile satellite networks (Louis, 2008). Considering a lossless (ideal) antenna with a physical aperture area $A\,(m^2)$, the gain of the ideal antenna with physical aperture area is defined as (Louis, 2008);

$$G_{ideal} = \frac{4\pi A}{\lambda^2} \quad (2.18)$$

Where; λ is the wavelength (meters) of the radio wave.

Physical antennas are not ideal as some energy is reflected away by the structure, and some energy is absorbed by lossy components (feeds, struts, sub-reflectors) (Louis, 2008). To account for these, an effective aperture, $A_e$is defined in terms of aperture efficiency, η_A such that:

$$A_e = \eta_A A \quad (2.19)$$

Where;A_e = Effective aperture, η_A = Aperture efficiency, A = Aperture area.

Antenna gain in dB for satellite applications is usually expressed as the dB value (Louis, 2008);

$$G(dB) = 10\log\ 109.66 f^2 d^2 \eta_A \quad (2.20)$$

Where; *d* = Physical diameter of the antenna, *f* = Carrier wave frequency.

2.2.14.4 Link Power Equation

The received power P_{ri} is commonly referred to as carrier power; because most satellite links use either frequency modulation for analog transmission or phase modulation for digital transmission (Ogundele, 2010). In both of these modulation systems, the amplitude of the carrier is not changed when the data are modulated onto the carrier.(Ogundele, 2010).

To compute the received power at the satellite receiver input, the isotropic power , gain of the satellite antenna G_{sat} and any receiver feeder losses rfl must to be taken into account (Adria, 2010);

$$P_{ri} = EIRP - tpl + G/T - rfl \quad dBW \quad (2.21)$$

Where; $EIRP$ = Effective Isotropic Radiated Power, *tpl* = Transmission path loss. G/T = Figure of Merit and *rfl* = Receiver feeder loss.

2.2.14.5 Figure of Merit

The figure of merit (G/T ratio) is another parameter of interest in link budgeting used to specifying the system performance(Dennis, 2001). The quality or efficiency of the receiver portions of a satellite communication link is often specified by a figure of merit; defined as a

ratio of antenna gain to system noise temperature(Dennis, 2001). The G/T is a singular parameter for measure of the performance of the receiver system, and is analogous to EIRP as the single parameter measure of performance for the transmitter of the link; mathematically presented as (Dennis, 2001);

$$[G/T]_{Uplink} = G_{sat} - T_s \quad (measured\ in\ dBK^{-1}) \tag{2.22}$$

Where, G = Antenna gain of the satellite and T_s = System noise temperature.

2.2.14.6 Carrier to Noise Density Ratio

Carrier to noise density ratio $\left(\frac{C}{N_O}\right)$is the ratio of the average wideband carrier power to noise density. Mathematically, carrier to noise density ratio is expressed as (NIIT, 2007);

$$\left[\frac{C}{N_o}\right] = EIRP - tpl + G_{sat} - T_s + 228.6\ (dB) \tag{2.23}$$

Where; $tpl = Lf + pl + aml + aal + Gal + Rl + fl + sl + tp$; with each parameter having its usual meaning as defined in equation (2.8).

2.2.14.7 Energy-Per-Bit to Noise Density

For digital communication systems, the bit energyE_b, is more useful than the carrier power in describing the performance of the link; and energy is related to the carrier power by the following equation (Ogundele, 2010);

$$E_b = CT_b \tag{2.24}$$

Where,C is the carrier power and T_b is the bit duration in seconds. The energy per bit to noise density is (Ogundele, 2010);

$$\frac{E_b}{N_o} = \mathrm{T_b}\left(C/N_o\right) = 1/R_b\left(C/N_o\right) \tag{2.25}$$

substituting equation 2.23 into 2.25 we have

$$E_b/N_o = [EIRP] - [\text{tpl}] + [G_r] + 228.6 - [T_s] - [R_b] \tag{2.26}$$

Where;Gt = transmitter antenna gain. Gr = receiver antenna gain;

R_b = System data rate; Pt = transmitting power.

The system data rate R, in bps (bits per second) depends on the code rate and the information data rate. The code rate or efficiency of a Forward Error Correction (FEC) code, such as a convolutional

code, can be expressed as a fractional number, k/n, meaning that, once the information is encoded, a n-bit codeword for every k-bit data word will be produced (Ogundele, 2010). In spite of not having fixed code rates, usually for convolutional codes, code rates of 1/2, 2/3, 3/4, etc, are used (Adria, 2010).

2.2.14.8 Overall Conventional Link Budget

It is worthy to note that in conventional approach to satellite link budget analysis, the effect of Doppler frequency shift is neglected as it can be seen in equations (2.23) and (2.26). Furthermore, a complete communication system consists of an uplink and downlink; and the overall C/N_0 ratio is the combine effect of these two (Vijitha et al, 2011). The carrier to noise ratio component of the uplink gives the carrier to noise power ratio for the link from the transmit terminal to the satellite receiver, and the carrier to noise ratio component of the downlink gives the carrier to noise power ratio for the link from the satellite antenna output to the ground receiver (Vijitha et al, 2011). The overall C/N_0 or C/N is expressed as: (Vijitha et al, 2011).

$$\left[C/N_0\right]_{Total} = \left[\frac{C}{N_0}\right]_{Uplink} + \left[\frac{C}{N_0}\right]_{Dowlink} \quad (2.27)$$

2.2.14.9 Link Margin

The Link Margin (*LM*) compares received C/N_0 or E_b/N_0 with that required for the established BER. The link margin will finally be:

$$LM = \left[\frac{C}{N_o}\right]_{received} - \left[\frac{C}{N_o}\right]_{required} \quad or \quad \left[\frac{E_b}{N_o}\right]_{received} - \left[\frac{E_b}{N_o}\right]_{required} \quad (2.28).$$

2.2.14.10 Radio Frequencies Bands

The radio frequency band is the range of frequencies that are transmitted through space. The modulated signal is converted from the intermediate frequency regime to the radio frequency regime by frequency translation. The RF frequencies typically range from a few hundred to a few thousand kilohertz for terrestrial broadcasting and from 1 to 30 gigahertz for satellite communication as shown in Table 2.1(Maral, 2002)

Table 2.1: Frequency Bands used in Satellite Communication (Maral, 2002)

Frequency band	Frequency range (GHz)
L – Band	1 – 2
S – Band	2 – 4
C – Band	4 – 8

X – Band	8 – 12
Ku – Band	12 – 18
K – Band	12 – 27
Ka – Band	27 – 40
V – Band	40 – 60
Millimeter	40 – 300

2.2.14.10.1 L band (1-2GHz)

This is used by Global Positioning System (GPS) carriers and also satellite mobile phones, such as Iridium; Inmarsat providing communications at sea, land and air; World Space satellite radio (Maral, 2002).

2.2.14.10.2 S-band(2–4GHz)

This is used by weather radar, surface ship radar, and some communications satellites, especially those of NASA for communication with International Space Station(ISS) and Space Shuttle (Maral, 2002).

2.2.14.10.3 C-band (4–8 GHz)

Satellite communication in this band is primarily used for, for full-time satellite TV networks or raw satellite feeds; commonly used in areas that are subject to tropical rainfall, because it is less susceptible to rainfade than Ku band (Maral, 2002).

2.2.14.10.4 X-band (8–12 GHz)

Communication in this band is primarily used for military application. It is used in radar applications including continuous-wave, pulsed, single-polarization, dual- polarization, synthetic aperture radar and phased arrays. X-band radar frequency sub-bands are used in civil, military and government institutions for weather monitoring, air traffic control, maritime vessel

traffic control, defense tracking and vehicle speed detection for law enforcement (Maral, 2002).

2.2.14.10.5 Ku-band (12–18 GHz)

Ku-band downlink is used from 10.7 GHz to 12.75 GHz for direct broadcast satellite services, such as Astra in most parts of Europe (Maral, 2002).

2.2.14.10.6 Ka - band

The Ka band uplink uses frequencies between 27.5GHz and 31GHz and the downlink uses frequencies between 18.3 and 18.8Ghz and between 19.7 and 20.2Ghz. The Ka band is branch of the K band from the electromagnetic spectrum. Ka band dishes can be much smaller thanC band dishes. Ka band dishes vary from 2′ to 5′ in diameter(Maral, 2002).

2.2.14.11 Modulation

Most modern satellite systems have moved away from the traditional frequency modulation (FM) schemes to FSk, *M*-ary PSK, and *M*-ary QAM or their variations(Johnson, 2005). The most common form of modulation in digital communication is M-ary Phase Shift Keying (PSK), evidently because of its simplicity and flexibility and therefore, considered as the heart of communication systems especially QPSK (Quadrature Phase Shift Keying).QPSK findsapplication in the area of remote data acquisition, measurement and control (Johnson, 2005).The expression for QPSK is given by (Maral, 2002):

$$S_i = Acos(2\pi f_t + \varphi_i) \qquad 0 \le t \le k_s \, i = 1,2,3,...,M \qquad (2.29)$$ Where;

$$\phi_i = \frac{(2i-1)\pi}{M} \qquad (2.30)$$

A = Signal amplitude, ϕ_i = Modulating phase, f_t = Carrier frequency,

K_s = Symbol duration and M = is the possible binary combinations representing thesignal state.

QPSK is usually preferred over BPSK because for a given bit rate and BER it requires the same power, yet requires only half the bandwidth (NIIT, 2007). The saving in bandwidth using QPSK instead of BPSK without any greater power is the digital communication synonymous to having a "free lunch". Essentially, the actually tradeoff is the increase in complexity the modulating device((Jamalipour, 1997).Therefore, until recently, QPSK has been the preferred form of digital modulation in satellite communications(Jamalipour, 1997).

2.3 REVIEW OF SIMILAR RESEARCH WORK

This section presents a critical review of some key research works carried out and published by researchers in similar area.

Khairi, (2009) presented satellite link margin prediction and performance of ASTRO Malaysia. In this paper, a link budget prediction tool for analyzing and comparing predicted and measured C/N and E_b/N_0 using a typical link margin and transmission availability was developed using MATLAB. The results obtained thereof, were compared with the performance of the actual signal quality measured at ASTRO uplink facility at Malaysia. However, limitations like Doppler frequency shift and atmospheric drag were not taken into account in evaluating satellite link budget.

Andrew *et al.,* (2010)investigated methods of exploiting the communication link of small satellites that are required to use fixed data rates. By choosing an appropriate data rate, total data downloaded can be maximized. In conjunction with global pass coverage analysis, the methods presented can help designers plan for optimal placement of ground stations and the optimal fixed data rate to use for the ground stations planned. The concepts presented, alter the normal mission planning strategy for small spacecraft communication links and were not representative enough to achieve the overall desired link budget for LEO.

Nikolaos Tsakalozos *et al.,* (2010) considered the Doppler effect as a channel in itself and not necessarily as impairment.The authors derived the input-output model for the Doppler effect in both a classical and a relativistic setting. The relativistic model, in particular, was derived in two independent ways, one kinematic based on the Minkowski diagram, the other through relativistic electrodynamics. The two derivations yielded consistent mathematical channel models. Furthermore, the relativistic model was shown, to give rise to the classical model when the speeds of the transmitter and the receiver are much smaller than the speed of light, or, equivalently, when the light is considered to propagate at infinite speed. The authors also examined the nature of the frequency shift, the Doppler effect induces, and they reaffirmed that, although in principle it is undoubtedly multiplicative, it can be considered to be additive with a good degree of approximation under the “narrowband assumption”, for most practical purposes. Their work followed a mathematical treatment of the Doppler Effect without necessarily considering its direct contribution to overall link budget of the communication system.

Dennis, (2010)presented the requirement, analysis and design used in LEONIDAS microsatellite project. Satellite tool kit software and Jan King link budget excel spread sheet was used create a link budget for the mission. The author considered the following parameters while designing the link

budget: orbit parameters, downlink frequency, uplink frequency cable lengths, antenna gain, and antenna pointing loss and modulation/demodulation methods. However, due to high amount of frequency offsets at LEO, it is necessary to include Doppler frequency shift effect in the link budget in other to produce a robust and accurate link budget.

Mehdi et al., (2010) investigated the advantages of using adaptive bit rate in the communication link of a Low Earth Orbit(LEO) satellite. During the research, the authors assumed that there was a communication subsystem on-board responsible for gathering the information sent by a number of ground data collection platforms. The subsystem which operates based on Store-And-Forward (SAF) scenario, contains two communication links, one for receiving data from ground platforms (Store case), and the other for forwarding the stored data to an Earth station (Forward case). The results obtained for a sample LEO (data collecting) satellite showed that utilizing adaptive bit rate instead of fixed bit rate can increase the daily data exchange up to 100%. However, the authors applied the scheme solely to a data collecting LEO satellite link thus rendering the concept of satellite link budget presented in the paper inadequate simply for not being representative enough to achieve a robust and accurate link budget and no validation was done.

Shkelzen *et al.,*(2011)presented antenna noise temperature for Low Earth Orbiting satellite ground stations at L and S Band. In this paper, the calculation and comparison of antenna noise temperature, caused under the worst propagation case, of the hypothetical satellite ground station implemented in different cities of Europe is given, inclusive of a Downlink link budget presentation. The observed drawback in the downlink link budget considered, proposed by the authors is not a true representation of link budgeting as the author s did not consider the uplink budget . A complete link budget is the summation of both the uplink and the downlink. In addition to this, the satellite link was only subjected to rain attenuation on antenna temperature which in itself does not account for the total losses encountered on satellite link.

Mebrek *et al.,* (2012) conducted a comparative study on link budget for systems operating in Ka band. The authors divided their research work in two parts; the first part, a system was designed for the study which consisted of a transmitting earth station, a receiver and a satellite. Secondly, they developed a computer based application (software) that enables the link budget calculation of any satellite. The software was then used to check the feasibility of implementing the proposed parameter. The results showed a margin error of 8.17dB excluding atmospheric disturbances such as rain and Doppler frequency shift. If thesedisturbances were included, the effects on the results would have been highly obtrusive.

Marie Rieche *et al.,* (2014)worked on the modeling of land mobile satellite channel considering the terminal's driving direction. It considered the channel between a satellite and a mobile terminal, which is of crucial importance while designing a satellite-based communication system especially in the case where the terrestrial based receiver is moving. The channel parameters used in modeling the land mobile satellite were not detailed enough to design a robust link. For instance, perturbations such as Doppler frequency shift effect, atmospheric drag which make orbit prediction and link budget design complex were neither used nor mentioned.

Snehasis *et al.*,(2014)presented a data sheet approach to calculate the performance and link budget of LEO satellite (Iridium) for communications operated at the frequency range 1650 - 1550MHz. The experimental results show that iterative techniques are needed to find a set of parameters for earth stations and the satellite, that provide the performance/link budget for a satellite communication system. The methodology presented and the iterative techniques were not representative enough to achieve the overall desired link budget for LEO. For example, the Doppler Frequency Shift, atmospheric drag which is an important parameter was not included in the set of parameters chosen in the data sheet.

Snehasis & Barsha, (2014)also presented a data sheet approach to calculate the performance and link budget of LEO satellite (Sky Bridge) communication operated at Ku band frequency range (12-14)GHz. The main aim of their research work was to prepare a link budget (with minimum limitation and maximum advantages) for LEO (Sky Bridge) satellite at (12-14)GHz frequency in a much simply way which will find its application in the present mobile communication systems. The experimental results show that iterative techniques must be used to find a set of parameters for earth stations and the satellite, that provide the performance/link budget for a satellite communication system. The methodology presented and the iterative techniques were not representative enough to achieve the overall desired link budget for LEO.

Yousif & Nor, (2014)presented a comparative system study of link budget analysis for underwater communication with the attenuation of the underwater channel using the same principle as RF link budget by means of modeling in the Matlab environment. The acoustic link budget incorporates terms of the active sonar equation to provide a first order estimate of signal available at the receiver. A more accurate link budget analysis operating at 15-20 kHz would not ignore the effect of Doppler frequency shift on the communication link as the author did considering the fact that both the satellite and the underwater equipments are both in motion.

In view of the shortcomings identified in the reviewed literature, This research work is aimed to improve the LEO-based satellite link budget of a land mobile communication systems by incorporating perturbation due to Doppler frequency shift into the link budget equation.

CHAPTER THREE

DESIGN METHODOLOGY

3.1 INTRODUCTION

The summary of methodology used for this research work has been presented in chapter one. This chapterpresents a step by step procedures and an in depth analysis leading to the more reliable approach to the estimation of satellite link budget.Comparison between the link budget modeled with Doppler effect and the conventional link budget analysis without the Doppler effect will be presented.

3.2 Selection of Key Parameters

Selections of key parameters such as carrier frequency, satellite transmitter power and methods of modulation and demodulation are described briefly below.

3.2.1 *Selection of Carrier Frequency*

The operating frequency of the transmission link is the critical factor in determining the type and severity of impairments introduced by the Earth's atmosphere. In order to reduce the complexity of analysis involving tedious computations, center frequencies of the various frequency bands (L, S, C, X Ku, K and Ka band) were selected as shown in Table 3.1. The computation Doppler frequency shift frequency was further simplified by narrowing it down to Ku, K and Ka bands. Ku, K and Ka frequency bands are used in this research work because broad band is becoming an issue due to the saturation of L, S and C frequency bands. Ku, K and Ka band provide the advantage of wider channel that support a greater number of user and it also allows the reducing of the size of antenna.

Table 3.1: Central Values of Frequency Bands

Frequency Band (Central Values)	Frequency range (GHz)	Center Frequency (GHz)
L – Band	1 – 2	1.5
S – Band	2 – 4	3.0
C – Band	4 – 8	6.0
X – Band	8 – 12	10.0
Ku – Band	12 – 18	15.0
K – Band	12 – 27	19.5
Ka – Band	27 – 40	33.5
V – Band	40 – 60	50.0
Millimeter	40 – 300	170.0

3.2.2 *Selection of the Satellite Transmitter Power*

The high power amplifier (HPA) in an earth station facility provides the RF carrier power to the input terminals of the antenna that, when combined with the antenna gain, yields the

equivalent isotropic radiated power (EIRP) required for the uplink to the satellite. The output power ratings of different HPA (KPA, SSPA and TWTA) are provided in Table 3.2. For the purpose of this research work, Traveling Wave Tube Amplifier (TWTA) is used due to its linearity,efficiency and reliability.The TWTAs also gives the widest bandwidth, with the best power consumption at a cost effective price when compared to KPA and SSPA.

Table 3.2: Power ratings of HPA (KPA, SSPA and TWTA) operating at Ku, K and Ka-bands (www.ATIcourses.com)

Type of Higher Power Amplifier (HPA)	Frequency Band (GHz)	Output Power (W)	Gain (dB)
KPA	Ku	10W-60W	45dB
	K	10W-100W	80dB
	Ka	15W-250W	80dB
SSPA	Ku	10W-100W	60dB 60dB
	K	10W-120W	60dB
	Ka	10W-120W	
TWTA	Ku	10W-700W	40Db
	K	10W-700W	40dB
	Ka	10W-700W	40dB

3.2.3 *Selection of Methods of Modulation and Demodulation*

The methods of modulation and demodulation used in this dissertation employ the technique of Quaternary Phase Shift Keying (QPSK).The selection of this scheme is due to the fact that for a given bit rate, the same power is required for both modulation and demodulation with 50% less of the channel bandwidth.

3.4 Development of a Mathematical Model of Doppler Frequency Shift

Doppler frequency shift could be best computed from the geometry of the satellite dynamic in orbit. Figure 3.1 was used to develop an appropriate mathematical representation of Doppler shift as the satellite sweeps over the orbit in an elliptical path.

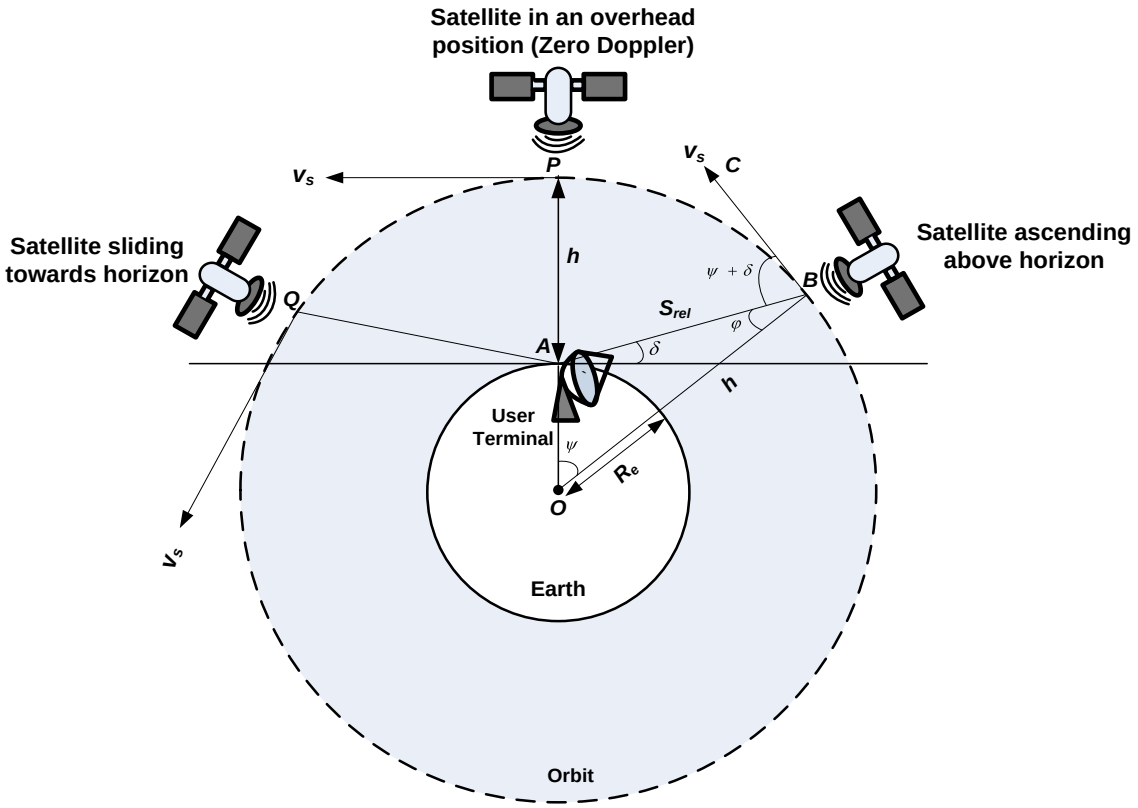


Figure 3.1: Geometrical Representation of Satellite Orbital Dynamics

Figure 3.1 is a modification of Figure 2.2, showing respectively the elevation angle (δ) , satellite coverage angle (ψ) and beam-width (tilt or nadir angle) of the satellite (φ) . It can be recalled from equation (2.14) that the Doppler shift frequency is given by;

$$f_{ds} = \frac{\vec{V}_{rel} f_c}{C} \tag{3.1}$$

f_{ds} = Doppler shift frequency, $\vec{V}_{rel}$ = relative velocity of the satellite and the Earth's terminal sometimes called relative radial velocity between the satellite and the Earth's, f_c = Carrier frequency and C =speed of light. Applying sine rule to ΔAOB in Figure 3.1, (δ) and (φ) are related to Earth radius (R_e) and height of the orbit (h) by the following equation;

$$\frac{\sin(90^0 + \delta)}{R_e + h} = \frac{\sin\varphi}{R_e} \tag{3.2}$$

Hence, $\sin\varphi = \dfrac{R_e \cos\delta}{R_e + h}$ (3.3)

Similarly, $\varphi = 90^0 - (\psi + \delta)$ (3.4)

Using equations (3.3) and (3.4), the satellite coverage angle ψ will be;

$$\psi = \cos^{-1}\left(\frac{R_e \cos\delta}{R_e + h}\right) - \delta \quad (3.5)$$

Where $(\psi + \delta)$ is the angle between the satellite and the line joining it with the Earth's terminal.

To compute the relative velocity between the satellite and the Earth's terminal, a radial vector component of the satellite velocity ($\vec{V}_{rel}$) in the direction relative to the Earth's terminal is obtain by the transformation of satellite velocity V_s along line AB of Figure 3.1 (lining joining the satellite and Earth's terminal).

$$\vec{V}_{rel} = V_S \cos(\psi + \delta) \quad (3.6)$$

Where V_S is the satellite orbital velocity. Using equation (3.5), equation (3.6) becomes;

$$\vec{V}_{rel} = V_S \sin\varphi \quad (3.7)$$

Substituting equation (3.3) in equation (3.7), the satellite radial velocity relative to the Earth's 1terminal becomes;

$$\vec{V}_{rel} = \frac{V_S R_e \cos\delta}{R_e + h} \quad (3.8)$$

Substituting equation (3.8) in equation (3.1), the Doppler shift frequency is written as;

$$f_{ds} = \frac{V_S R_e f_c \cos\delta}{C \;\; R_e + h} \quad (3.9)$$

It can be seen from equation (3.9) that the Doppler shift is zero when the grazing or elevation angle, δ is equal to 90^0 . In this position, the satellite is directly overhead the Earth's terminal. The relative distance between the satellite and the Earth's terminal S_{rel} is calculated from the cosine rule using Δ AOB as;

$$S_{rel} = \left[R^2{}_e + \left(R_e + h \right)^2 - 2R_e \left(R_e + h \right) \cos\psi \right]^{1/2} \tag{3.10}$$

Similarly, S_{rel} can be calculated from sine rule as;

$$\frac{S_{rel}}{\sin\psi} = \frac{R_e + h}{\sin(90^0 + \delta)} \tag{3.11}$$

$$\cos\delta = \left(\frac{R_e + h}{S_{rel}} \right) \sin\psi \tag{3.12}$$

Using equation (3.12), equation (3.9) is further expressed as;

$$f_{ds} = \frac{V_S R_e f_c \sin\psi}{C S_{rel}} \tag{3.13}$$

The magnitude of the velocity of satellite in orbit is calculated from law gravitation as (Carassa, 1989 and Valdoni, 1990);

$$V_S = \frac{2\pi \left(R_e + h \right)}{T} \tag{3.14}$$

Where T is the satellite orbital period.

The period of the satellite can be calculated from Kepler's equation as (Valdoni, 1990);

$$T = 2\pi \sqrt{\frac{\left(R_e + h \right)^3}{\mu_L}} \tag{3.15}$$

Equation (3.14) can also be written as;

$$V_S = \sqrt{\frac{\mu_L}{R_e + h}} \tag{3.16}$$

Where $\mu_L = 398\,600\, km^3 \sec^{-2} = 3.896 \times 10^{14} m^3 \sec^{-2}$ (Kepler's constant).

It can be seen from equations (3.10) through (3.16) that the Doppler frequency shift depends on both the relative velocity and distance between the satellite and Earth's terminal, the frequency of the carrier signal, the height of the orbit, the period of satellite on the orbit and it contribute to the total loss on a transmission link particularly in LEO .Doppler frequency shift can be expressed in dB using equation (3.13) as follows;

$$f_{ds} = \left[10\log\ V_S R_e f_c \sin\psi\ \right] - \left[10\log\ CS_{rel}\ \right]\ (dB) \qquad (3.17)$$

3.4.1 *Effect of the Earth's (User) Terminal Location on Doppler Frequency*

Doppler frequency varies as the location of the user terminal changes. This effect is analytically analysed from the geometry of the satellite and user terminal position shown in Figure 3.2.

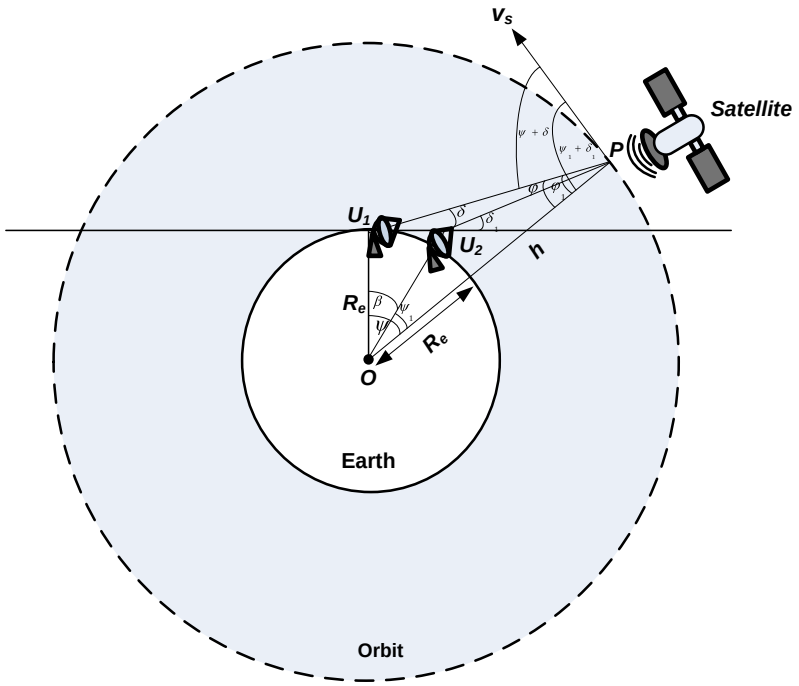


Figure 3.2: Geometry of the Earth's Terminal Location

Suppose the User moves from point U_1 to U_2 through an angle β , the distance traveled is equal to the length of arc $U_1 U_2$ given by;

$$\beta = \frac{U_1 U_2}{R_e}\ (\beta\ measured\ in\ radian) \qquad (3.18)$$

Therefore, the new satellite coverage angle becomes;

$$\psi_1 = \psi - \beta \qquad (3.19)$$

3.5 Development of a Modified Model of a Satellite Link Budget by Including Doppler Effect

The modified model of link budget is obtained by adding the Doppler equation in decibel to the classical link budget equation (equations (2.23) and (2.26)). The modified link budget equation is expressed as;

$$\left[\frac{C}{N_o}\right]_{Modified} = EIRP - fsl + pl + aml + aal + Gal + Rl + fl + sl + tp - f_{ds} + G_{sat} - T_s + 228.6 \quad (3.20)$$

Where; $f_{ds} = \left[10\log V_S R_e f_c \sin\psi\right] - \left[10\log CS_{rel}\right]\ (dB)$ and $tpl = fsl + pl + aml + aal + Gal + Rl + fl + sl + tp$. Therefore equation (3.20) becomes

$$\left[\frac{C}{N_o}\right]_{Modified} = EIRP - tpl - f_{ds} + G_{sat} - T_s + 228.6 \quad (3.21)$$

As an illustration, Doppler effect was calculated at minimum grazing or elevation angle and the corresponding maximum satellite coverage angle, $(\delta_{\min} = 20.07^0 \ and \ \psi_{\max} = 8^0)$ (Carassa, 1989) using the following values:

$V_S = 7377.57\,ms^{-1}$, $R_e = 6378km$, $h = 780km$, $f_c = (15.0GHz, 19.5GHz \ and \ 33.5GHz)$ and $S_{rel} = 2480.54km$. Using these values and equation (3.13), the Doppler frequency shift for Ku, K and Ka bands in LEO were respectively calculated as: f_{dsku}=325.483kHz, f_{dsk}=423.129kHz and f_{dska}=726.914kHz.The corresponding values of these frequencies in decibel are: $f_{dsKu} = 55.125\ (dB)$, $f_{dsK} = 56.265\ (dB)$ and $f_{dsKa} = 58.615\ (dB)$. With these values, modified link budget equations at Ku, K and Ka bands can be respectively written as;

$$\left[\frac{C}{N_o}\right]_{Modified(Ku)} = EIRP - tpl + G_{sat} - 55.125 - T_s + 228.6\ (dB) \quad (3.22)$$

$$\left[\frac{C}{N_o}\right]_{Modified(K)} = EIRP - tpl + G_{sat} - 56.265 - T_s + 228.6\ (dB) \quad (3.23)$$

$$\left[\frac{C}{N_o}\right]_{Modified(Ka)} = EIRP - tpl + G_{sat} - 58.615 - T_s + 228.6\ (dB) \quad (3.24)$$

Recall from equation (2.15), $EIRP = P_t + G_t$, therefore, modified equation for energy per noise density, $\left[\frac{E_b}{N_0}\right]$ using equations (2.26) including the Doppler effect becomes;

$$\left[E_b/N_o\right] = Pt + Gt + Gr - tpl - f_{ds} + 228.6 - T_s - R_b \quad (3.25)$$

Therefore, the overall link budget equations taking into account the effect of Doppler in terms of $\frac{C}{N_0}$ and $\frac{E_b}{N_0}$ both up ink and down link can be written as;

$$\left[C/N_o\right]_{Up\ link} = Pt_{ET} + Gt_{ET} + Gr_{Sat} - tpl - f_{ds} + 228.6 - T_{Sat} \quad (3.26)$$

$$\left[C/N_o\right]_{Down\ link} = Pt_{Sat} + Gt_{Sat} + Gr_{ET} - tpl - f_{ds} + 228.6 - T_{ET} \quad (3.27)$$

$$\left[E_b/N_o\right]_{Up\ link} = Pt_{ET} + Gt_{ET} + Gr_{Sat} - tpl - f_{ds} + 228.6 - T_{Sat} - \left[R_{b\uparrow}\right] \quad (3.28)$$

$$\left[E_b/N_o\right]_{Down\ link} = Pt_{Sat} + Gt_{Sat} + Gr_{ET} - tpl - f_{ds} + 228.6 - T_{ET} - \left[R_{b\downarrow}\right] \quad (3.29)$$

The total carrier to noise density ratio is the summation of equations (3.26) and (3.27). Similarly, the summation of equations (3.28) and (3.29) yields the total energy bit to noise density ratio. The two parameters are expressed as;

$$\left[C/N_o\right]_{Total} = [Pt]_{ET} + [Gt]_{ET} + [Gr]_{sat} + [Pt]_{sat} + [Gt]_{sat} + [Gr]_{ET} - [T_{sat}] - [T_{ET}] - 2([tpl] + [f_{ds}]) + 457.2 \quad (3.30)$$

$$\left[E_b/N_o\right]_{Total} = [Pt]_{ET} + [Gt]_{ET} + [Gr]_{sat} + [Pt]_{sat} + [Gt]_{sat} + [Gr]_{ET} - [T_{sat}] - [T_{ET}] - 2([tpl] + [f_{ds}]) - [R_{b\uparrow}] - [R_{b\downarrow}] + 457.2 \quad (3.31)$$

3.6 MODIFIED LINK MODEL VALIDATION

The modified model developed was validated using the work of Snehasis & Barsha (2014)as reference point. The modified model was tested with the same parameters used by Snehasis &Barsha as shown in Table 3.3. The choice of Snehasis & Barsha (2014) as a means of validation is based on the fact that it is the most recent work available to the best of my knowledge. Moreover, the work has presented a simple but yet detailed conventional approach to link budget analysis in the LEO orbit in the Kuband. The table parameters is used for validation (Snehasis & Barsha, 2014).

Table 3.3: Satellite Link Budget Parameters (Snehasis & Barsha, 2014)

S/N	General Data	Symbol	Value
1	Carrier Frequency	F_c	12-14 GHz
2	Transmitting Power	$(P_{tx})_{Up}$	10 dB
		$(P_{tx})_{Down}$	7 dB
3	Transmitted Gain	$(G_{tx})_{Up}$	3 dB
		$(G_{tx})_{Down}$	3 dB
4	Binary Rate	R_b	120 MBPS
5	Bandwidth	*BW*	91.761dBHz
6	Operating Temperature	*T*	290 K
7	Boltzmann's Constant	*K*	-228.6 dB
8	Atmospheric Loss	*La*	1 dB
9	Polarization Losses	*Lp*	3 dB
10	Antenna Misalignment Loss	*Lant*	1 dB
11	Loss due to rain Attenuation	*Rl*	0.1 dB
12	Free Space Loss	$(fsl)_{Up}$	118.365 dB
		$(fsl)_{Down}$	117.365 dB

13	Total Path Loss	$(tpl)_{Up}$	123.465 dB
		$(tpl)_{Down}$	122.365 dB
14	Figure of Merit	G/T	-21.624 dB
15	Effective Isotropic Radiated Power	$(EIRP)_{Up}$	30 dBW
		$(EIRP)_{Down}$	21 dBW
16	Received Power	$(P_r)_{Up}$	-107.704 dB
		$(P_r)_{Down}$	-98.365 dB
17	Carrier to Noise Ratio	$(C/N)_{UP}$	21.512 dB
		$(C/N)_{Down}$	13.851 dB
18	Total Carrier to Noise Ratio	$(C/N)_{Total}$	35.363 dB

3.7 CONCLUSION

The mathematical model of Doppler shift on satellite link budget was developed and modified model of satellite link budget was presented. The developed model wasverified and validated through comparison with the work of Snehasis & Barsha (2014).

CHAPTER FOUR

RESULTS AND ANALYSIS

4.1 INTRODUCTION

Following the analyses on the modification of satellite link budget model with the effect of Doppler shift frequency, this chapter focuses on the interpretation of the results based on the analyses presented in the preceding chapter.

4.2 VARIATION OF DOPPLER FREQUENCY WITH ORBITAL HEIGHT

The fact that Doppler effect is much more pronounced in LEO than in both MEO and GEO is investigated in this section. Using equations (3.10) , (3.16) and minimum grazing or elevation angle with its corresponding maximum satellite coverage angle $(\delta_{\min} = 20.07^0 \ \ and \ \ \psi_{\max} = 8^0)$ (Carassa, 1989), Doppler frequency shift was plotted against the orbital height for different earth's orbits at different frequency bands (Ku, K and Ka) as shown in Figure 4.1.

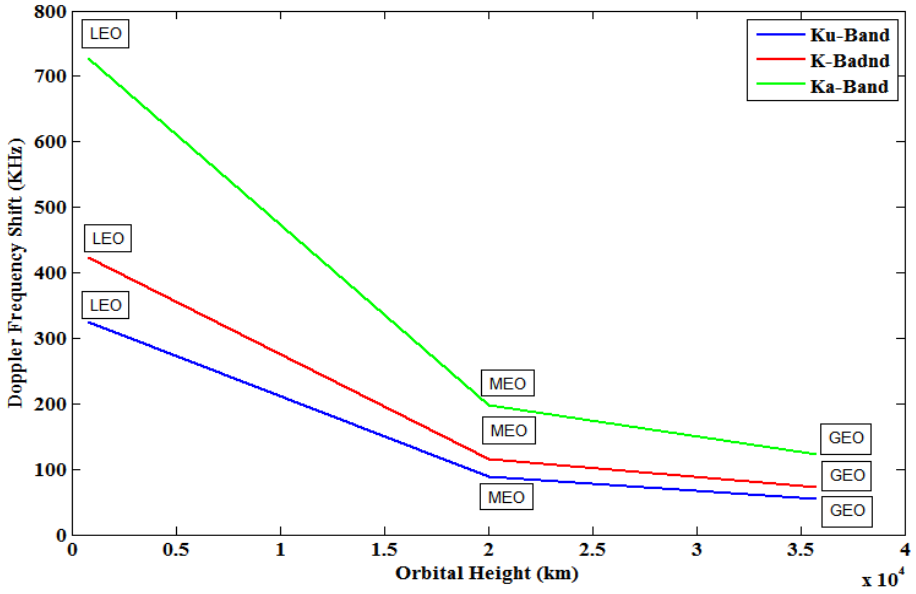


Figure 4.1: Variation of Doppler Frequency with Orbital Height.

As it can be seen from Figure 4.1, there is a sharp decrease in Doppler frequency shift as the height of the orbit increases form LEO through MEO to GEO. This phenomenon is further summarized in Table 4.1.

Table 4.1: Variation of Doppler Frequency with Orbital Height

Type of Orbit	Doppler Frequency (*KHz*)		
	Ku-band	K-band	Ka-band
LEO (780 km)	325.50	423.20	726.90
MEO (20000 km)	88.33	114.80	197.30
GEO (35786 km)	55.26	71.84	123.40

The difference in Doppler Frequencies between LEO and MEO, LEO and GEO are: 237.17 *kHz* and270.24 *kHz* respectively at Ku-band. At K-band, these differences are 308 *kHz* and 351.36 *kHz*. At Ka-band, the Doppler frequency differences are respectively 529.6 *kHz* and 603.5 k*Hz*. From the foregoing therefore, it can be concluded that Doppler effect is much more sever in LEO than both in MEO and GEO. Having established the effect of Doppler frequency shift in LEO, its variation with respect to the relative distance between satellite and the Earth's terminal for different elevation angles ($0^0 - 90^0$) at Ku, K, and Ka bands was also investigated using equations (3.10) – (3.13); and is depicted in Figure 4.2.

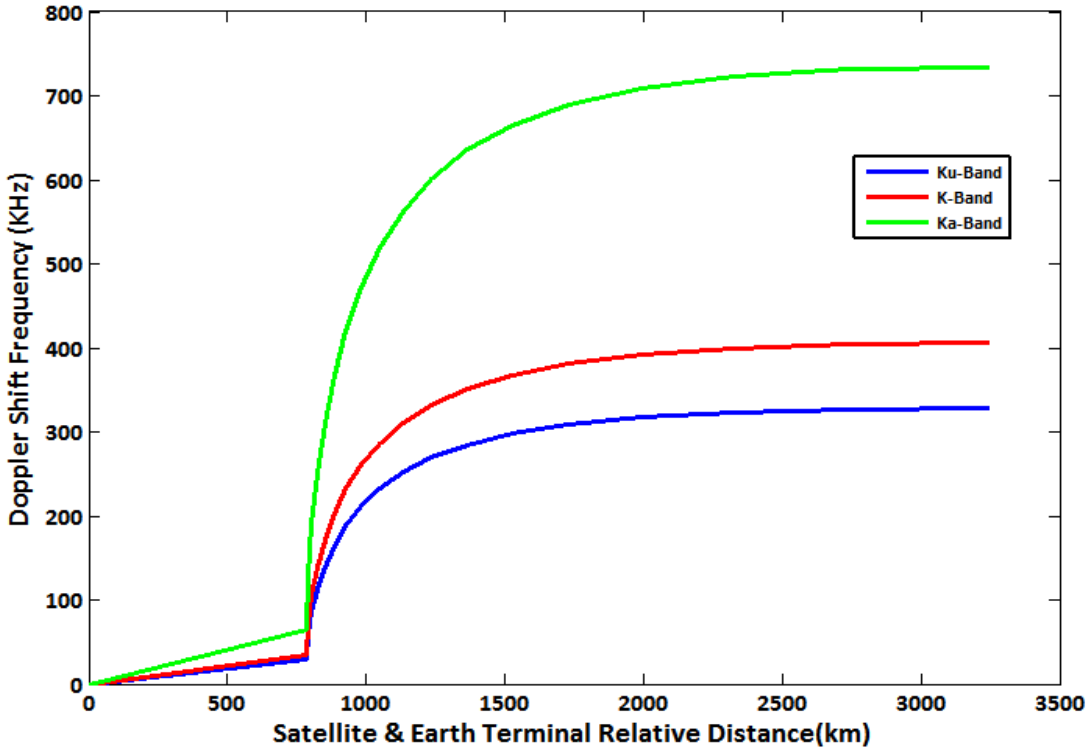


Figure 4.2: Variation of Doppler Frequency with the Satellite and Earth's Relative Distance

It can be seen form Figure 4.2 that between 0-790 km, Doppler frequency increases linearly with the satellite and earth's terminal (user terminal) relative distance. However, beyond this distance, a positive nonlinear increase in Doppler frequency was observed. This is due to continuous change in azimuth angle of the satellite position with respect to the earth's station. Moreover, using Figure 4.2, the Doppler frequency has the highest value of 325.485 kHz at Ku-band, 401.09 kHz at K-band and 745.89 kHz at Ka-band.

4.3 EFFECT OF USER TERMINAL LOCATION ON DOPPLER FREQUENCY

Knowing the new position of the Earth's terminal, the new relative distance between the satellite and the Earth's station can be calculated. Similarly, the deviation in Doppler frequency from the initial estimated value can also be determined. Equations (3.5), (3.10), (3.13), (3.18) and (3.19) were used to graphically (see Figure 4.3) show the effect of the location of earth's terminal on Doppler frequency.

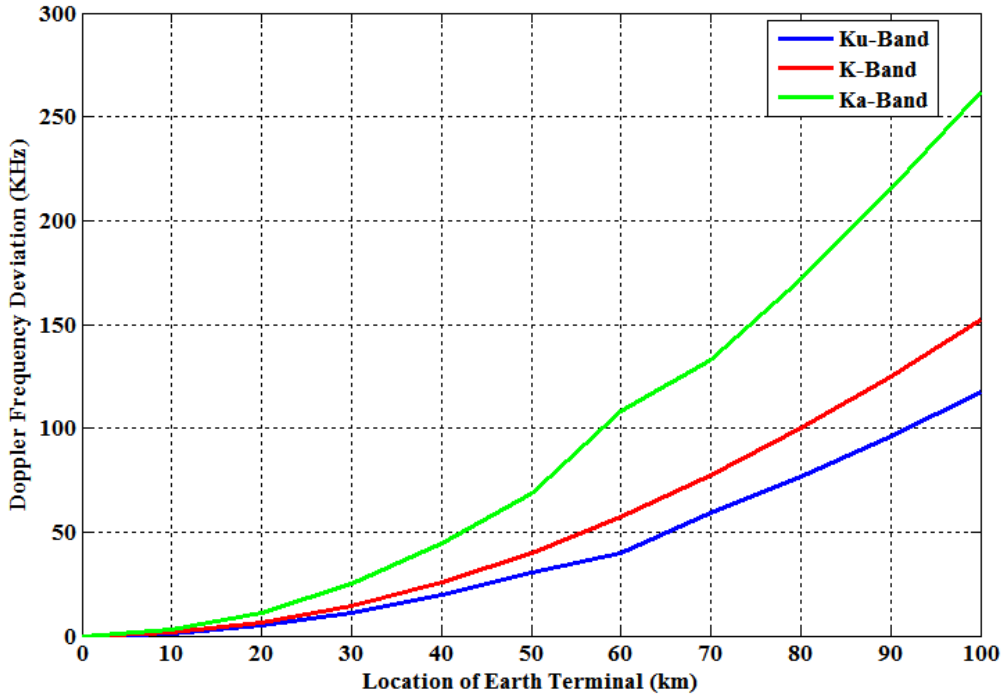


Figure: 4.3: Variation of Doppler Frequency with Distance.

Figure 4.3 shows that the Doppler effect increases with the increase in distance from the initial location of the user terminal. 0 km -100 km was assumed to be the range of distance of user terminal from his the initial to final locations inclusive.

4.4 VARIATION OF CARRIER TO NOISE DENSITY RATIO WITH TRANSMISSION PATH LOSS

In order to investigate the effect of Doppler frequency shift on the carrier signal, the overall carrier to noise density ratio was plotted against the total transmission path loss at Ku, K and Ka bands with and without the Doppler frequency shift. This relationship is depicted in Figures: 4.4, 4.5and 4.6; which were obtained using equations: (2.23), (2.27), (3.30), (3.20) and the data in Table 3.2.

4.4.1 Variation of Carrier to Noise Density Ratio with Transmission Path Loss at Ku-Band

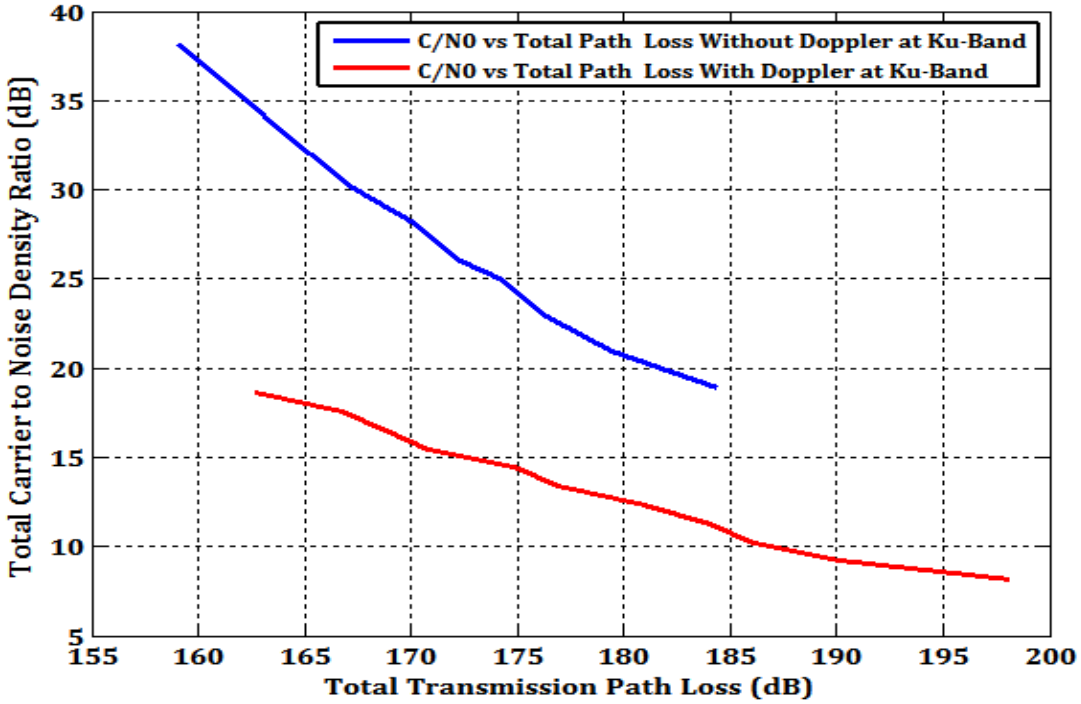


Figure 4.4: C/N_0 against the Transmission Path Loss at Ku-Band

From Figure 4.4 it can be seen that there is considerable decrease incarrier to noise density ratio. When the Doppler frequency shift was introduced, an appreciable decrease in C/N_0 was observed. At 175 dB transmission path lossfor instance,

the Carrier to Noise density ratio C/N_0 for Ku frequency banddropped by 40% (from 25dB without Doppler shift to 15dB with Doppler shift).

4.4.2 Variation of Carrier to Noise Density Ratio with Transmission Path Loss at K-Band

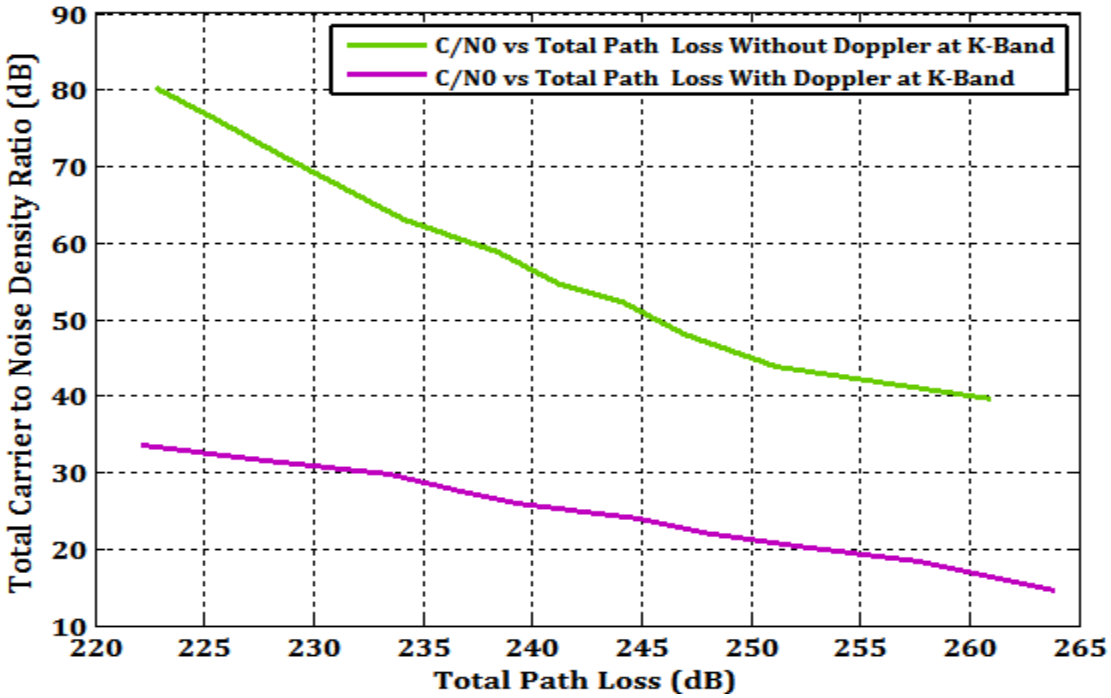


Figure 4.5: C/N_0 against the Transmission Path Loss at K-Band

From Figure 4.5, At K band, a considerable reduction in carrier to noise density ratio, C/N_0 is seen. At 230 dB transmission path loss for instance, the C/N_0 for K frequency banddropped by 57% (from 70dB without Doppler shift to 30dB with Doppler shift).

4.4.3 Variation of Carrier to Noise Density Ratio with Transmission Path Loss at Ka-Band

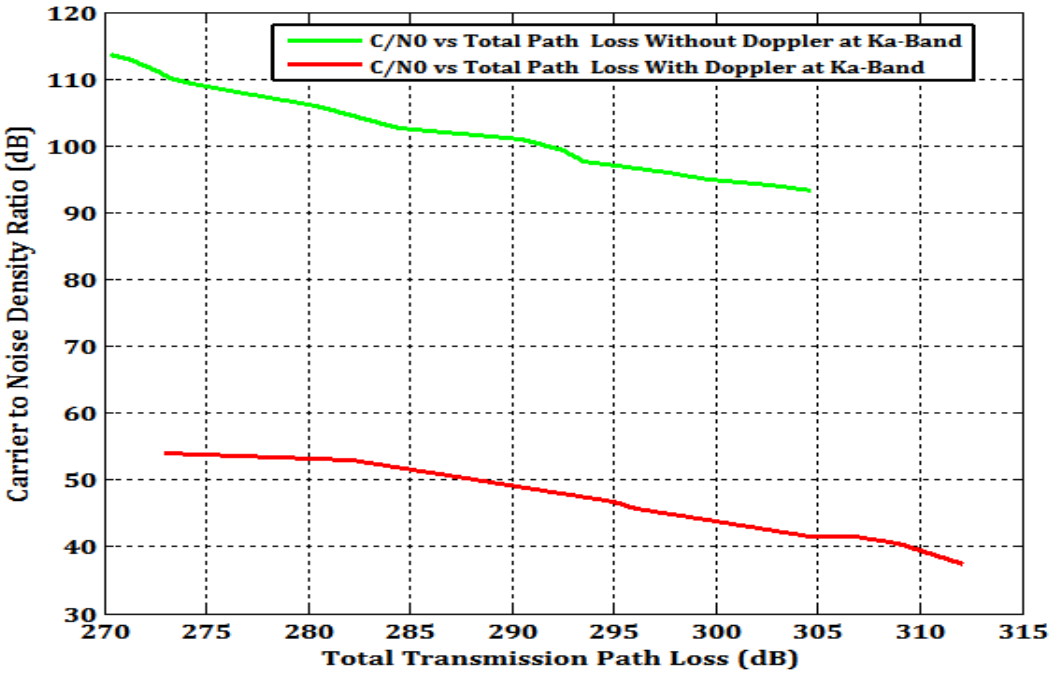


Figure 4.6: C/N_0 against the Transmission Path Loss at Ka-Band.

As it is illustrated in Figure 4.6 the carrier to noise density ratio droppedby 52% at 275dB transmission path loss (from 110dB without Doppler shift to 53dB with Doppler shift).

4.5 MODIFIED LINK MODEL VALIDATION RESULTS

The modified model developed was validatedthrough comparison with the work of Snehasis &Barsha (2014).

The developed model was compared with the conventional model which utilized data found in Table 3.3. For the conventional link budget model, equations 2.23 and 2.27 were used. Similarly equations 3.30 and 3.20 were used in creating the developed model. The graphical plots obtained thereof were juxtaposed in Figures 4.7, 4.8 and 4.9. These figures (4.7, 4.8 and 4.9) further confirmed that with the inclusion of impairment due to Doppler frequency shift, there was a significant decline in carrier to noise density ratio when compared withthe corresponding values obtained without the Doppler frequency effect (using conventional model).

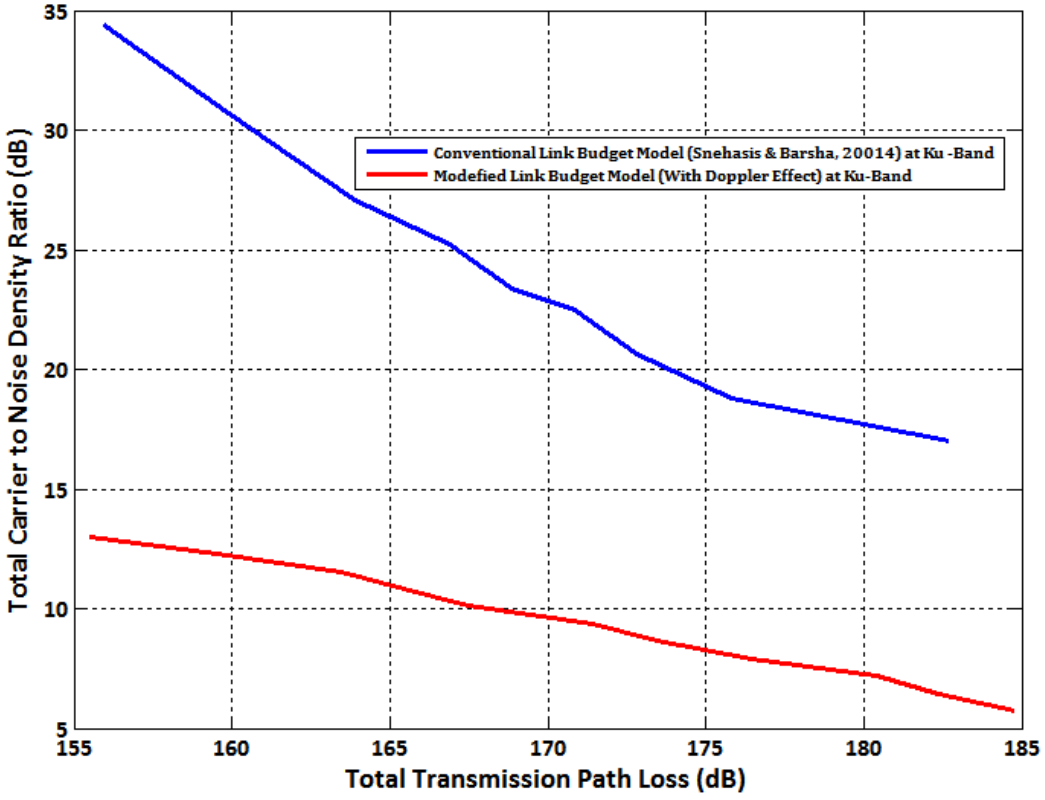


Figure 4.7: Variation of $^{C}/_{N_0}$ with Transmission Path Loss at Ku-Band

From Figure 4.7, it can be seen that at transmission path of 160dB for example, the Carrier to Noise density ratio $^{C}/_{N_0}$ for Ku frequency banddropped by 58% (from 31dB without Doppler shift to 13dB with Doppler shift).

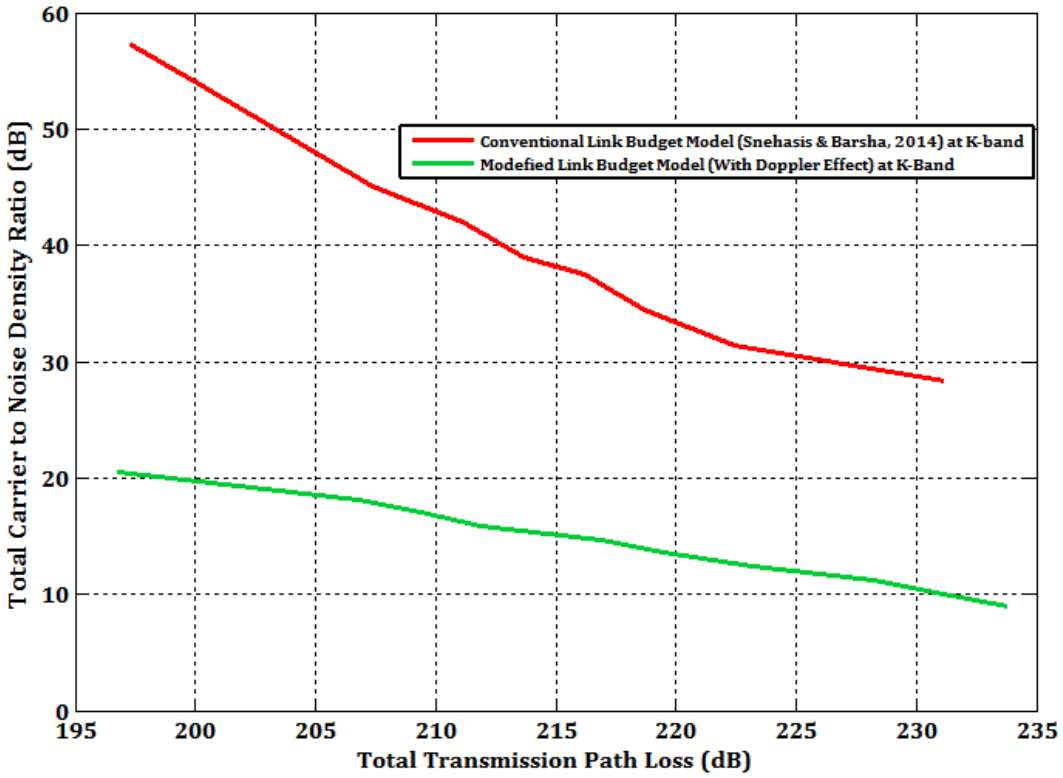


Figure 4.8: Variation of $^{C}/_{N_0}$ with Transmission Path Loss at K-Band

At K band, a considerable reduction in carrier to noise density ratio , $^{C}/_{N_0}$ is seen. The $^{C}/_{N_0}$ for K frequency bandat 200dB transmission path loss dropped by 62% (from 54dB without Doppler shift to 20dB with Doppler shift).

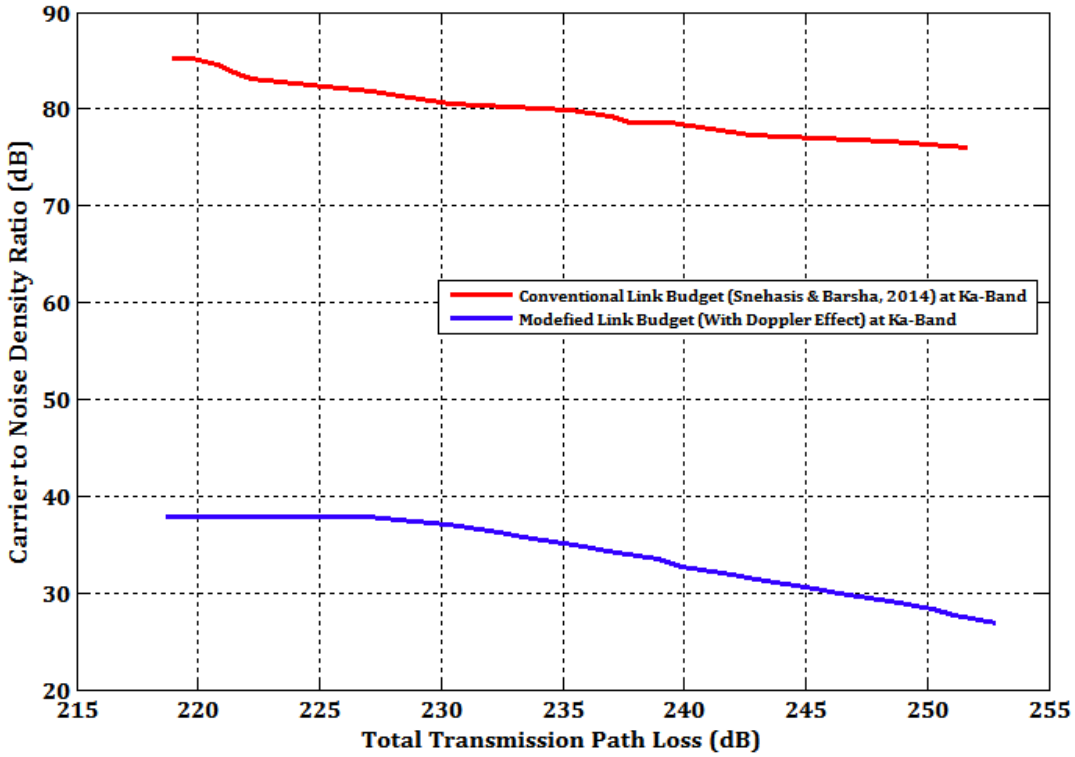


Figure 4.9: Variation of $^{C}/_{N_0}$ with Transmission Path Loss at Ka-Band

The results at Ka band follows a similar pattern when compared with that observed in the Ku and K band. The $^{C}/_{N_0}$ for Ka frequency band dropped by 55% (from 85dB without Doppler shift to 38dB with Doppler shift).

4.6 CONCLUSION

Comparisons between the link budget modeled with Doppler effect and the conventional link budget without the Doppler effect has been presented and validated. The modified satellite link model was simulated and the results obtained were then validated through comparison with the same data used by Snehasis & Barsha, 2014 who did not consider Doppler shift effect. The results obtained show the Carrier to Noise density ratio $^{C}/_{N_0}$ for Ku frequency banddropped by 58% (from 31dB without Doppler shift to 13dB with Doppler shift). The $^{C}/_{N_0}$ for K frequency band dropped by 62% (from 54dB without Doppler shift to 20dB with Doppler shift). The results at Ka band follows a similar pattern when compared with that observed in the Ku and K band. The $^{C}/_{N_0}$ for Ka frequency band dropped by 55% (from 85dB without Doppler shift to 38dB with Doppler shift).

This clearly shows that the effect of Doppler shift which is often overlooked is critical in the evaluation of link budgetin a LEO-based satellite communications system.

CHAPTER FIVE

CONCLUSION AND RECOMMENDATION

5.1 INTRODUCTION

In this chapter the summary of the research contribution is presented. The summary of the entire thesis is captured in the conclusion. The work in this dissertation has been limited to the development of a modifiedLow Earth Orbiting (LEO)-based link budget for land mobile satellite communications system operating at Ku, K and Ka frequency bands by considering the effect of additional loss due to Doppler frequency shift.

5.2 CONCLUSIONS

A detailed approach to the development of modified link budget for land mobile satellites communication systems was presented. The model took into account the additional impairment due to Doppler frequency shift, which is often neglected in the conventional satellite link budget model. The effect of losses due to Doppler frequency shift on satellite link budget was investigated at different satellite orbits (LEO, MEO and GEO). The results obtained show that at maximum satellite converge angle and central frequencies for Ku, K and Ka bands, the Doppler frequencies for LEO (780 km) were: 325.50 kHz, 423.20 kHz and 726.90 kHz; MEO (20000 km) had: 88.33 kHz, 114.80 kHz and 197.30 kHz; while GEO (35786 km) had 55.26 kHz, 71.84 kHz and 123.40 kHz. Variation of Doppler frequency shift with respect to the latitude (location) of the earth's terminal relative to the satellite

motion was also studied. A typical earth terminal location in the range of0 km – 100 km was selected for the study; from which it was verified that effect of Doppler shift in LEO increased as the distance from the initial location of the user terminal increased. These results further confirm that, Doppler effect is more pronounced in LEO than in MEO and GEO. Comparative analyses between the conventional (without Doppler shift) and the modified link budget (with the inclusion of Doppler shift) at Ku, K and Ka bands was achieved thereof. The results obtained show the Carrier to Noise density ratio C/N_0 for Ku frequency banddropped by 58% (from 31dB without Doppler shift to 13dB with Doppler shift). The C/N_0 for K frequency band dropped by 62% (from 54dB without Doppler shift to 20dB with Doppler shift). The results at Ka band follows a similar pattern when compared with that observed in the Ku and K band. The C/N_0 for Ka frequency band dropped by 55% (from 85dB without Doppler shift to 38dB with Doppler shift). It can be seen from the results obtained that with Doppler shift, Carrier to noise density ratio is worse when compared to the values obtained by snehasis and Barsha.

5.3 SIGNIFICANT CONTRIBUTIONS OF THE RESEARCH

A lot of work has been done in the area of prediction and analysis of mobile satellite link budget using the conventional approach. The results of this approach are unrealistic because it, does not take into consideration the effect of Doppler shift variable in the link budget analysis for Low Earth Orbit (LEO). In view of this, the following are some of the contributions this research has made to the concept of link budgeting:

i. A comprehensive mathematical model of Doppler effect on link budget was developed and its effect on earth's terminal location in relation to the position of satellite on LEO was also looked into. A typical earth terminal location in the range of 0 km – 100 km was selected for the study and was verified that the effect of Doppler shift on link budget in LEO increased as the distance from the initial location of the user terminal increased and also confirmed that Doppler effect is more pronounced in LEO than in MEO and GEO.

ii. The fact that Doppler frequency shift is much more pronounced in LEO than in both MEO and GEO at Ku, K, and Ka bands were investigated and graphically presented. The results obtained show a sharp decrease in Doppler frequency shift as the height of the orbit increased from LEO through MEO to GEO. It was found out that, at maximum

satellite converge angle and central frequencies for Ku, K and Ka bands, the Doppler frequencies for LEO (780 km) were: 325.50 kHz, 423.20 kHz and 726.90 kHz;

MEO (20000 km) had: 88.33 kHz, 114.80 kHz and 197.30 kHz; and GEO (35786 km) with 55.26 kHz, 71.84 kHz and 123.40 kHz.

iii. Comparative analyses results of conventional (without Doppler shift) and the modified link budget (with the inclusion of Doppler shift) approaches at Ku, K and Ka bands showed that the Carrier to Noise density ratio C/N_0 for Ku frequency banddropped by 58% (from 31dB without Doppler shift to 13dB with Doppler shift).The C/N_0 for K frequency band dropped by 62% (from 54dB without Doppler shift to 20dB with Doppler shift). The C/N_0 for Ka frequency band dropped by 55% (from 85dB without Doppler shift to 38dB with Doppler shift).

5.4 RECOMMENDATIONS FORFURTHER WORK

The following are the recommendations for further works:

i. Effect of interference due to neighbouring orbiting satellite should be considered in the link budget.

ii. The perturbation effect due to atmospheric dragon LEO orbiting satellites should also be considered.

REFERENCES

Andrew, T., & JamesCutler, W.(2010).Exploiting the Link: Improving Satellite Communication Through Higher Elevation Links.*AIAA/AAS Astrodynamics Specialist Conference (p. 8269).*

Andria Ainhoa, S. E. (2010).Front-End Design for a Multi-Mission, Multi-Standard Satellite Ground Station (Doctoral dissertation), *Institut für Nachrichtentechnik und Hochfrequenztechnik).pp 53, 55.*

Asoka Dissanayake, (2002). Ka band propagation modeling for fixed satellite applications. *Online Journal of Space Communication*

Burdic, W. S. (1984). Underwater acoustic system analysis. *Prentice Hall.pp5*

Carassa, F. (1989). Application of millimeter waves to satellite systems. *Alta Frequenza*, *pp58, 485-489.*

Dennis, D.(2010).Telecommunication subsystem requirements, analysis and design. *Interfaces*, *8*, 1.

Dennis, R.(2002).Satellite communications*,The McGraw Hill Companies, Inc. pp 328, 348*

Gataullin Y., Dikanskis, D., Häusler M., Wiedemann K., Albrecht N., Engelhardt W., & Strauss, G.(2010). Selection of functional operational requirements for the new 13-M DLR Ka band ground station in Weilheim.*International Workshop on Tracking, Telemetry and Command Systems for Space Applications.*

Jamalipour A. (1997).Low earth orbital satellites for personal communication networks.*Artech House, Inc..pp51-52*

Johnson I. Ejimanya (1991) Communication Electronics. Springfield publishers. http/www.Springfieldpublishers.com

Khairi Abdul Rahim., Mahamod Ismail., & Mardina Abdullah(2009). Satellite link margin prediction and performance of astro malaysia. *Proceeding of the 2009 international conference on space and communication.*

Kausik M., Bera R. N., & Sil, S. (2007). An Estimation of Doppler Frequency due to Moving Object Like Rain and Others to find its Remedial Measures from a Microwave Communication System.*Proc. NCDCTC'07*.

Levanon N. (1988).Radar principles. *New York, Wiley-Interscience, p.1*

Louis J. Ippolito(2008). Satellite communications systems engineering: atmospheric effects, satellite link design and system performance. *John Wiley & Sons. pp61-67, 72*

Maral G., & Bousquet, M. (2002). Satellite Communications Systems, *Antony Rowe Ltd., Chippenham, Wiltshire, Great Britain.*

Marie Rieche., Alexander Ihlow., daniel A., Fernando P., & Giovanni Del Galdo (2014).Modeling of the land mobile satellite channel considering the terminal's driving direction. *International Journal of Antennas and Propagation*, *2015*

Mebrek M.A., Abdeeeahmanen Himeur A., & Bendokha (2012). Configuration and the calculation of link budget for the connection via a geostationary satellite for multimedia application in the ka band. *World academy of science, engineering and technology journal. vol:6.*

Mehdi Hosseini., Mohammad Halkkak., & Pejman Rezaei (2010).Adaptive bit rate scheme for a LEO satellite link.*Electrical Engineering (ICEE), Iranian Conference (pp. 200-203). IEEE.*

Naser Ayat & Mohamad mehdipour (2001). Accurate Doppler Prediction Scheme for Satellite Orbits. Computer engineering group, Payam Noor University

NIIT (2007).,Advanced Digital Communication Systems.*Prentice-Hall of India Private Limited, pp 124, 133-134, 525-542*

Nikolaos Tsakalozoz., Konstantonos Drakakis., & Scott Rickard (2010) Channel models of the Doppler effect:*Adv. studies Theor. phys., Vol.4, no.2, 67-90*

Ogundele A. Daniel., (2010).Understanding Satellite communications. *Siddwell Productions Companies.pp51, 52-57*

Pratt T., Charles B., & Jeremy A., (2003**).** Satellite communications.*John Wiley & Sons*

Qingchong. L. (1999). Doppler measurement and compensation in mobile satellite communications systems. *In Military Communications Conference Proceedings, 1999. MILCOM 1999. IEEE (Vol. 1, pp. 316-320). IEEE.*

Ray E., Sherrif., & Fun Hu., (2000).Mobile satellite communication Networks.*John Wiley and sons Ltd.*

Raymond P. L., (1996). Communications by means of low Earth orbiting satellites. *Modern Radio Science*, 133-149.

Seybold John S., (2005)Introduction to RF Propagation.*John Wiley & Sons*.

Shkelzen Cakaj., Bexhet Kamo., Indrit Enesi., & Olimpjon Shurdi(2011). Antenna noise temperature for low earth orbiting satellite ground stations at L and S band.*the third international conference on advances in satellite and space communications.*

Shkelzen Cakaj., Bexhet Kamo., Algenti Lala & Alban Rakipi (2014).The Coverage Analysis for Low Earth Orbiting Satellites at Low Elevation. *Editorial Preface*, *5*(6).

Shkelzen Cakaj., Kresimir malaric & Arpad Scholtz (2008). Modeling of interference caused by uplink signal for low earth orbiting satellite ground stations. *Proceeding of the 17th IASTED international conference Applied simulation and modelling*.

Snehasis D., & Barsha B.S. (2014)Link budget of LEO Satellite (Sky Bridge) for communication operated at Ku band frequency range (12- 14)GHz.*International Journal of innovations in engineering and Technology (IJIET), Vol.4, Issue 1*

Snehasis, D., Deepak K.M., & Satya, D.R., (2014). An Approach to calculate the Performance and Link Budget of Leo satellite (Iridium) for communication operated at frequency range (1650-1550)MHz. *International Journal of innovations in engineering and Technology (IJIET), Vol 4, Issue 1. pp 96-103*

Valdoni F., Ruggieri M., Vatalaro F., & Paraboni A. (1990). A new millimetre wave satellite system for land mobile communications. *European Transactions on Telecommunications*, *1*(5), 533-544.

Vijitha Weerackody., & Enrique Cuevas (2011). Technical challenges and performance of satellite communications on the move systems. *John Hopkins APL technical digest, Volume 30.*

Williams O.P., & Xie, Y. (1999). Propagation characterization of LEO/MEO satellite systems at 900-2100 MHz. *Wireless Communications and Systems, 2000. 1999 Emerging Technologies Symposium* (pp. 21-1). IEEE.

Yousif M.H., & Nor H.K, (2014)Link Budget Analysis for underwater communication system.*The international journal of Electrical and Electronic Research, Vol.2, Issue 4, pp 195-200*

You M. H., Lee, S. P., & Han, Y. (2000). Adaptive Compensation Method Using the Prediction Algorithm for the Doppler Frequency Shift in the LEO Orbit Mobile Satellite Communication System. *ETRI journal*, *22*(4), 32-39.

Appendix A

THE MATLAB FUNCTION

print results to text file

```
clc

delta = [0:5:90]';
R_e = 6378 * 10^3;
mu_l = 3.896 * 10^14;
h = [780 20000 35786] * 10^3;
f_c = [15 18.5 33.5] * 10^9;
C = 3 * 10^8;

T = 2 * pi * sqrt(((R_e + h).^2) / mu_l);

V_s = sqrt(mu_l ./ (R_e + h));

for i=1:1:length(delta)
    psi(i,:)=acosd((R_e * cosd(delta(i))) ./ (R_e + h)) - delta(i);
    phi(i,:) = 90 - (psi(i,:) + delta(i));
    S_rel(i,:) = (R_e + h) .* (sind(psi(i,:)) / cosd(delta(i)));
    f_dsh1(i,:) = (V_s(1) .* R_e .* f_c .* sind(psi(i,1))) ./ (C * S_rel(i,1));
    f_dsh2(i,:) = (V_s(2) .* R_e .* f_c .* sind(psi(i,2))) ./ (C * S_rel(i,2));
    f_dsh3(i,:) = (V_s(3) .* R_e .* f_c .* sind(psi(i,3))) ./ (C * S_rel(i,3));
end
```

```
fileID = fopen('minister_work.txt', 'w');

fprintf(fileID, '%12s %12s %12s\r\n', 'T_1', 'T_2', 'T_3');
fprintf(fileID, '%12.4f %12.4f %12.4f\r\n\r\n\r\n', T);

fprintf(fileID, '%12s %12s %12s\r\n', 'V_s1', 'V_s2', 'V_s3');
fprintf(fileID, '%12.4f %12.4f %12.4f\r\n\r\n\r\n', V_s);

fprintf(fileID, '%6s %12s %12s %12s\r\n', 'delta', 'psi_1', 'psi_2', 'psi_3');
fprintf(fileID, '%6.0f %12.4f %12.4f %12.4f\r\n', [delta, psi]');
fprintf(fileID, '\r\n\r\n');

fprintf(fileID, '%6s %12s %12s %12s\r\n', 'delta', 'phi_1', 'phi_2', 'phi_3');
fprintf(fileID, '%6.0f %12.4f %12.4f %12.4f\r\n', [delta, phi]');
fprintf(fileID, '\r\n\r\n');

fprintf(fileID, '%6s %16s %16s %16s\r\n', 'delta', 'S_rel1', 'S_rel2', 'S_rel3');
```

```
fprintf(fileID, '%6.0f %16.4f %16.4f %16.4f\r\n', [delta, S_rel]');
fprintf(fileID, '\r\n\r\n');

fprintf(fileID, 'f_ds for h1\r\n');
fprintf(fileID, '%6s %16s %16s %16s\r\n', 'delta', 'f_ds1', 'f_ds2', 'f_ds3');
fprintf(fileID, '%6.0f %16.4f %16.4f %16.4f\r\n', [delta, f_dsh1]');
fprintf(fileID, '\r\n\r\n');

fprintf(fileID, 'f_ds for h2\r\n');
fprintf(fileID, '%6s %16s %16s %16s\r\n', 'delta', 'f_ds1', 'f_ds2', 'f_ds3');
fprintf(fileID, '%6.0f %16.4f %16.4f %16.4f\r\n', [delta, f_dsh2]');
fprintf(fileID, '\r\n\r\n');

fprintf(fileID, 'f_ds for h3\r\n');
fprintf(fileID, '%6s %16s %16s %16s\r\n', 'delta', 'f_ds1', 'f_ds2', 'f_ds3');
fprintf(fileID, '%6.0f %16.4f %16.4f %16.4f\r\n', [delta, f_dsh3]');
fprintf(fileID, '\r\n\r\n');

fclose(fileID);

disp('I am done!')

type minister_work.txt

%no commment!
```

```
I am done!

         T_1          T_2          T_3
      2.2786       8.3968      13.4218


        V_s1         V_s2         V_s3
   7377.5749    3843.1607    3039.7549


 delta        psi_1        psi_2        psi_3
     0      26.9969      76.0076      81.2997
     5      22.4218      71.0620      76.3330
    10      18.6584      66.2244      71.4329
    15      15.6081      61.4936      66.5983
    20      13.1444      56.8671      61.8281
    25      11.1429      52.3416      57.1203
    30       9.4972      47.9129      52.4726
    35       8.1228      43.5762      47.8822
    40       6.9553      39.3258      43.3458
    45       5.9459      35.1556      38.8598
    50       5.0582      31.0588      34.4202
    55       4.2646      27.0282      30.0226
    60       3.5437      23.0562      25.6624
    65       2.8789      19.1349      21.3347
    70       2.2568      15.2563      17.0344
    75       1.6667      11.4121      12.7563
```

80	1.0991	7.5936	8.4948
85	0.5460	3.7925	4.2446
90	0.0000	0.0000	0.0000

delta	phi_1	phi_2	phi_3
0	63.0031	13.9924	8.7003
5	62.5782	13.9380	8.6670
10	61.3416	13.7756	8.5671
15	59.3919	13.5064	8.4017
20	56.8556	13.1329	8.1719
25	53.8571	12.6584	7.8797
30	50.5028	12.0871	7.5274
35	46.8772	11.4238	7.1178
40	43.0447	10.6742	6.6542
45	39.0541	9.8444	6.1402
50	34.9418	8.9412	5.5798
55	30.7354	7.9718	4.9774
60	26.4563	6.9438	4.3376
65	22.1211	5.8651	3.6653
70	17.7432	4.7437	2.9656
75	13.3333	3.5879	2.2437
80	8.9009	2.4064	1.5052
85	4.4540	1.2075	0.7554
90	0.0000	0.0000	0.0000

delta	S_rel1	S_rel2	S_rel3
0	3249319.9288	25595312.0708	41678819.7050
5	2740646.3933	25045468.3292	41126647.1536
10	2325356.7799	24511734.5672	40586004.1604
15	1993843.8124	23997740.7511	40060749.1129
20	1732239.0303	23506696.3798	39554461.8459
25	1526339.0039	23041391.7518	39070430.0706
30	1363779.4807	22604210.7540	38611642.7343
35	1234685.9707	22197153.3519	38180789.6497
40	1131516.0637	21821865.6816	37780266.5633
45	1048626.8982	21479675.5245	37412184.7046
50	981828.1296	21171630.9861	37078383.7857
55	928010.4000	20898540.3616	36780447.4029
60	884862.8571	20661011.4139	36519719.8102
65	850667.1318	20459488.5856	36297323.0961
70	824150.1654	20294286.9648	36114173.8823
75	804380.3899	20165622.1129	35970998.7646
80	790695.4668	20073635.1096	35868347.8388
85	782653.2051	20018412.3768	35806605.7713
90	0.0000	0.0000	0.0000

f_ds for h1

delta	f_ds1	f_ds2	f_ds3
0	328682.4021	405374.9626	734057.3647
5	327431.6663	403832.3885	731264.0548
10	323688.9779	399216.4060	722905.3839

15	317482.8208	391562.1457	709044.9665
20	308860.4278	380927.8610	689788.2888
25	297887.4205	367394.4853	665281.9058
30	284647.3100	351065.0157	635712.3257
35	269240.8616	332063.7293	601304.5909
40	251785.3277	310535.2375	562320.5652
45	232413.5554	286643.3850	519056.9404
50	211272.9756	260570.0032	471842.9788
55	188524.4809	232513.5264	421038.0073
60	164341.2011	202687.4813	367028.6824
65	138907.1854	171318.8620	310226.0475
70	112416.0023	138646.4028	251062.4051
75	85069.2655	104918.7607	189988.0262
80	57075.1002	70392.6235	127467.7237
85	28646.5589	35330.7560	63977.3148
90	0.0000	0.0000	0.0000

f_ds for h2

delta	f_ds1	f_ds2	f_ds3
0	46462.3527	57303.5684	103765.9211
5	46285.5494	57085.5110	103371.0604
10	45756.4852	56432.9984	102189.4836
15	44879.1864	55350.9966	100230.1831
20	43660.3300	53847.7403	97508.0703
25	42109.1921	51934.6702	94043.8623
30	40237.5778	49626.3459	89863.9237
35	38059.7312	46940.3352	85000.0664
40	35592.2271	43897.0801	79489.3072
45	32853.8447	40519.7418	73373.5865
50	29865.4246	36834.0237	66699.4484
55	26649.7107	32867.9765	59517.6872
60	23231.1764	28651.7842	51882.9605
65	19635.8387	24217.5345	43853.3732
70	15891.0605	19598.9747	35490.0352
75	12025.3418	14831.2548	26856.5966
80	8068.1029	9950.6602	18018.7631
85	4049.4609	4994.3351	9043.7959
90	0.0000	0.0000	0.0000

f_ds for h3

delta	f_ds1	f_ds2	f_ds3
0	22990.6519	28355.1374	51345.7893
5	22903.1656	28247.2375	51150.4031
10	22641.3723	27924.3591	50565.7314
15	22207.2645	27388.9595	49596.2240
20	21604.1460	26645.1134	48249.2593
25	20836.6069	25698.4818	46535.0887
30	19910.4886	24556.2693	44466.7579
35	18832.8395	23227.1687	42060.0083
40	17611.8612	21721.2954	39333.1566
45	16256.8459	20050.1099	36306.9558
50	14778.1062	18226.3310	33004.4372

```
    55       13186.8962       16263.8386       29450.7348
    60       11495.3260       14177.5687       25672.8947
    65        9716.2694       11983.3989       21699.6682
    70        7863.2661        9698.0281       17561.2942
    75        5950.4186        7338.8496       13289.2682
    80        3992.2848        4923.8179        8916.1027
    85        2003.7673        2471.3131        4475.0804
    90           0.0000           0.0000           0.0000
```

```
%% Computation of Dppler Frquency Shift in LEO for Ku, K and Ka Bands
delta = [0:5:90];
psi_1=[26.9969 22.4218 18.6584 15.6081 13.1444 11.1429 9.4972 8.1228 6.9553
5.9459 5.0582 4.2646 3.5437 2.8789 2.2568 1.6667 1.0991 0.5460 0.0000];
s_1=(1/1000)*[3249319.9288 2740646.3933 2325356.7799 1993843.8124
1732239.0303 1526339.0039 1363779.4807 1234685.9707 1131516.0637
1048626.8982 981828.1296 928010.4000 884862.8571 850667.1318 824150.1654
804380.3899 790695.4668 782653.2051 0.0000];
f_ds1=(1/1000)*[328682.4021 327431.6663 323688.9779 317482.8208 308860.4278
297887.4205 284647.3100 269240.8616 251785.3277 232413.5554 211272.9756
188524.4809 164341.2011 138907.1854 112416.0023 85069.2655 57075.1002
28646.5589 0.0000];
f_ds2=(1/1000)*[405374.9626 403832.3885 399216.4060 391562.1457 380927.8610
367394.4853 351065.0157 332063.7293 310535.2375 286643.3850 260570.0032
232513.5264 202687.4813 171318.8620 138646.4028 104918.7607 70392.6235
35330.7560 0.0000];
f_ds3=(1/1000)*[734057.3647 731264.0548 722905.3839 709044.9665 689788.2888
665281.9058 635712.3257 601304.5909 562320.5652 519056.9404 471842.9788
421038.0073 367028.6824 310226.0475 251062.4051 189988.0262 127467.7237
63977.3148 0.0000];
plot(delta,psi_1,'linewidth',2.5,'markersize',12);xlabel('Elevation Angle
(degrees)'); ylabel('Satellite Coverage Angle (degrees)');
plot(s_1,delta, 'linewidth',2.5,'markersize',12);xlabel('Satellite & Earth
Terminal Relative Distance(km)');ylabel('Elevation Angle (degrees)');
plot(s_1,f_ds1,'linewidth',2.5,'markersize',12);
hold on
plot(s_1,f_ds2,'r','linewidth',2.5,'markersize',12);
hold on
plot(s_1,f_ds3,'g','linewidth',2.5,'markersize',12);
xlabel('Satellite & Earth Terminal Relative Distance(km)');ylabel('Doppler
Shift Frequency (KHz)');legend('Ku-Band','K-Band','Ka-Band');
text(40,25,'Variation of Elevation Angle & Satellite Coverage Angle in LEO')

%% Computation of Dppler Frquency Shift in MEO for Ku, K and Ka Bands
psi_2=[76.0076 71.0620 66.2244 61.4936 56.8671 52.3416 47.9129 43.5762
39.3258 35.1556 31.0588 27.0282 23.0562 19.1349 15.2563 11.4121 7.5936
3.7925 0.0000];
s_2=(1/1000)*[25595312.0708 25045468.3292 24511734.5672 23997740.7511
23506696.3798 23041391.7518 22604210.7540 22197153.3519 21821865.6816
21479675.5245 21171630.9861 20898540.3616 20661011.4139 20459488.5856
20294286.9648 20165622.1129 20073635.1096 20018412.3768 0.0000];
f_ds21=(1/1000)*[46462.3527 46285.5494 45756.4852 44879.1864 43660.3300
42109.1921 40237.5778 38059.7312 35592.2271 32853.8447 29865.4246 26649.7107
```

```
23231.1764 19635.8387 15891.0605 12025.3418 8068.1029 4049.4609
0.0000];f_ds22=(1/1000)*[57303.5684 57085.5110 56432.9984 55350.9966
53847.7403 51934.6702 49626.3459 46940.3352 43897.0801 40519.7418 36834.0237
32867.9765 28651.7842 24217.5345 19598.9747 14831.2548 9950.6602 4994.3351
0.0000];
f_ds23=(1/1000)*[103765.9211 103371.0604 102189.4836 100230.1831 97508.0703
94043.8623 89863.9237 85000.0664 79489.3072 73373.5865 66699.4484 59517.6872
51882.9605 43853.3732 35490.0352 26856.5966 18018.7631 9043.7959 0.0000];
plot(s_2,f_ds21,'linewidth',2.5,'markersize',12);
hold on
plot(s_2,f_ds22,'r','linewidth',2.5,'markersize',12);
hold on
plot(s_2,f_ds23,'g','linewidth',2.5,'markersize',12);
xlabel('Satellite & Earth Terminal Relative Distance(km)');ylabel('Doppler
Shift Frequency (KHz)');legend('Ku-Band', 'K-Band','Ka-Band');
text(40,25,'Effect of Doppler Frequency Shift in MEO');

%% Computation of Dppler Frquency Shift in GEO for Ku, K and Ka Bands;
psi_3=[81.2997 76.3330 71.4329 66.5983 61.8281 57.1203 52.4726 47.8822
43.3458 38.8598 34.4202 30.0226 25.6624 21.3347 17.0344 12.7563 8.4948
4.2446 0.0000];
s_3=(1/1000)*[41678819.7050 41126647.1536 40586004.1604 40060749.1129
39554461.8459 39070430.0706 38611642.7343 38180789.6497 37780266.5633
37412184.7046 37078383.7857 36780447.4029 36519719.8102 36297323.0961
36114173.8823 35970998.7646 35868347.8388 35806605.7713 0.0000];
f_ds31=(1/1000)*[22990.6519 22903.1656 22641.3723 22207.2645 21604.1460
20836.6069 19910.4886 18832.8395 17611.8612 16256.8459 14778.1062 13186.8962
11495.3260 9716.2694 7863.2661 5950.4186 3992.2848 2003.7673 0.0000];
f_ds32=(1/1000)*[28355.1374 28247.2375 27924.3591 27388.9595 26645.1134
25698.4818 24556.2693 23227.1687 21721.2954 20050.1099 18226.3310 16263.8386
14177.5687 11983.3989 9698.0281 7338.8496 4923.8179 2471.3131 0.0000];
f_ds33=(1/1000)*[51345.7893 51150.4031 50565.7314 49596.2240 48249.2593
46535.0887 44466.7579 42060.0083 39333.1566 36306.9558 33004.4372 29450.7348
25672.8947 21699.6682 17561.2942 13289.2682 8916.1027 4475.0804 0.0000];
plot(s_3,f_ds31,'linewidth',2.5,'markersize',12);
hold on
plot(s_3,f_ds32,'r','linewidth',2.5,'markersize',12);
hold on
plot(s_3,f_ds33,'g','linewidth',2.5,'markersize',12);
xlabel('Satellite & Earth Terminal Relative Distance(km)');ylabel('Doppler
Shift Frequency (KHz)');legend('Ku-Band', 'K-Band','Ka-Band');
text(40,25,'Effect of Doppler Frequency Shift in GEO');

%% Comparison of Doppler Effect in LEO, MEO & GEO for Ku, K & Ka Frequency-
Bands
ylabel('Doppler Shift Frequency (KHz)'); text(40,25,'Effect of Doppler
Frequency Shift in Ku-Band')
plot(s_3,f_ds2,'b',s_3,f_ds22,'r',s_3,f_ds32,'g','linewidth',2,'markersize',
12);legend('LEO','MEO','GEO');
xlabel('Satellite & Earth Terminal Relative Distance(km)');
ylabel('Doppler Shift Frequency (KHz)'); text(40,25,'Effect of Doppler
Frequency Shift in K-Band');
plot(s_3,f_ds3,'b',s_3,f_ds23,'r',s_3,f_ds33,'g','linewidth',2,'markersize',
12);legend('LEO','MEO','GEO');
xlabel('Satellite & Earth Terminal Relative Distance(km)');
ylabel('Doppler Shift Frequency (KHz)'); text(40,25,'Doppler Frequency Shift
in Ka-Band')
```

```
%% Effect of the Location of Earth's Treminal on Doppler Frequency Shift
D=[0 10 20 30 40 50 60 70 80 90 100];
Delta=[0:5:50];
psi=[26.9969 22.3319 18.47874 15.33861 12.7851 10.6937 8.9582 7.4940 6.2366
5.1374 4.1599];
s=[3249.3189 2730.2233 2303.7469 1960.2494 1685.6883 1465.5377 1287.0289
1139.6704 1015.0912 906.4331 807.7981];
fds1=[0 1.25 4.99 11.19 19.82 30.79 40.04 59.44 76.89 96.27 117.40];
fds2=[0 1.63 6.49 14.56 25.77 40.03 57.25 77.27 99.97 125.15 152.63];
fds3=[0 2.79 11.15 25.01 44.27 68.78 107.83 132.75 171.74 215.00 262.21];
plot(D,s,'linewidth',2.5,'markersize',12);xlabel('Earth Terminal Location
km)');ylabel('Relative Distance between Satellite & Earth Terminal Location
(km)');
plot(D,fds1,'linewidth',2.5,'markersize',12);
hold on
plot(D,fds2,'r','linewidth',2.5,'markersize',12);
hold on
plot(D,fds3,'g','linewidth',2.5,'markersize',12);
xlabel('Location of Earth Terminal (km)');ylabel('Doppler Frequency
Deviation (KHz)');legend('Ku-Band','K-Band','Ka-Band');
text(50,200,'Variation of Doppler Frequency Deviation with the Position of
User Terminal');
plot(s_3,f_ds1,'b',s_3,f_ds21,'r',s_3,f_ds31,'g','linewidth',2,'markersize',
12);legend('LEO','MEO','GEO');
xlabel('Satellite & Earth Terminal Relative Distance(km)');

delta = 20.7;
R_e = 6378 * 10^3;
mu_l = 3.896 * 10^14;
h = 780.6 * 10^3;
C = 3 * 10^8;
V_s = sqrt(mu_l ./ (R_e + h));
fc_up_ku = [14:0.05:14.5]'*10^9;
fc_dn_ku = [11.7:0.05:12.2]'*10^9;
p_l = 3.0;   %% Loss due to Ploarization (dB)
R_l = 0.4;   %% Loss due to Rain Attenuation (dB)
aa_l = 0.8;  %% Loss due to Atmospheric Absorption (dB)
f_l = 0.02;  %% Loss due to Attenuation caused by Cloud or Fog (dB)
s_l = 0.008; %% Loss due to Attenuation caused by Snow (dB)
tp_l = 0.5;  %% Loss due to Scintillation of Troposphere and Ionosphere (dB)
am_l = 1.0;  %% Loss due to Antenna Misalignment(dB)
Ga_l = 0.18; %% Loss due to Gaseous Absorption (dB)
t_l = p_l + R_l  + aa_l + f_l + s_l + tp_l + am_l + Ga_l;
Pst = 10;    %% Satellite Power (W)
Gst = 40;    %% Satellite Antenna Gain (dB)
BWS = 30;    %% Transponder bandwidth (MHz)
Pet = 100;    %% Earth Station Power (W)
Get = 5.0;   %% Earth Station Gain (dB)
BWE = 1.5;   %% Earth Station Bandwidth (GHz)
Tet = 290;   %% Earthh Station Temperature (K)
Tst = 290;   %% Satellite Temperature (K)
Rc = 400;    %% Channel Data Rate (Coded) Foward Error Code (3/4) for QPSK
(kbps)
Rb = 25.67;  %% Channel Data Rare (Uncoded) (dB)
```

```
%%%% UpLink Satellite Link Budget at KU-Band

for i = 1:length(fc_up_ku)
for j = 1:length(fc_dn_ku)
fds_up_ku(i,:) = 10*log10((V_s*R_e*fc_up_ku(i)*cosd(delta))./(C*(R_e+h)));
%% Up link Doppler Frequency for ku-band
fs_l_up_ku(i,:) = 20*log10(4*pi*h*fc_up_ku(i)./C); %% Up link Free Space
Loss for ku
TPL_up_ku(i,:) = fs_l_up_ku(i,:) + t_l; %% Up link Transmission Path Loss
without Doppler for ku
TPLD_up_ku(i,:) = TPL_up_ku(i,:) + fds_up_ku(i,:); %% Up link Total
Transmission Path Loss with Doppler for ku
CN0D_up_ku(i,:) = 10*log10(Pet) + Get + Gst - TPLD_up_ku(i,:) -
10*log10(Tet) + 228.6; %% Up link Signal to Noise ratio for ku with Doppler
CN0_up_ku(i,:) = 10*log10(Pet) + Get + Gst - TPL_up_ku(i,:) - 10*log10(Tet)
+ 228.6; %% Up link Signal to Noise ratio for ku without Doppler

fds_dn_ku(j,:) = 10*log10((V_s*R_e*fc_dn_ku(j)*cosd(delta))./(C*(R_e+h)));
%% Down link Doppler Frequency for ku-band
fs_l_dn_ku(j,:) = 20*log10(4*pi*h*fc_dn_ku(j)./C); %% Down link Free Space
Loss for ku
TPL_dn_ku(j,:) = fs_l_dn_ku(j,:) + t_l; %% Down link Transmission Path Loss
without Doppler for ku
TPLD_dn_ku(j,:) = TPL_dn_ku(j,:) + fds_dn_ku(j,:); %% Down link Total
Transmission Path Loss with Doppler for ku
CN0D_dn_ku = 10*log10(Pst) + Gst + Get - TPLD_dn_ku(j,:) - 10*log10(Tst) +
228.6; %% Down link Signal to Noise ratio for ku with Doppler
CN0_dn_ku = 10*log10(Pst) + Gst + Get - TPL_dn_ku(j,:) - 10*log10(Tst) +
228.6; %% Down link Signal to Noise ratio for ku without Doppler
TCN0_ku = CN0_up_ku + CN0_dn_ku;
TCN0D_ku = CN0D_up_ku + CN0D_dn_ku;
%plot(TPL_up_ku(i,:), CN0_up_ku);
end
end

%%%% UpLink Satellite Link Budget at Ka-Band

for a = 1:length(fc_up_ka)
for b = 1:length(fc_dn_ka)
fds_up_ka(a,:) = 10*log10((V_s*R_e*fc_up_ka(a)*cosd(delta))./(C*(R_e+h)));
%% Up link Doppler Frequency for ka-band
fs_l_up_ka(a,:) = 20*log10(4*pi*h*fc_up_ka(i)./C); %% Up link Free Space
Loss for ka
TPL_up_ka(a,:) = fs_l_up_ka(a,:) + t_l; %% Up link Transmission Path Loss
without Doppler for ka
TPLD_up_ka(a,:) = TPL_up_ka(a,:) + fds_up_ka(a,:); %% Up link Total
Transmission Path Loss with Doppler for ka
CN0D_up_ka(a,:) = 10*log10(Pet) + Get + Gst - TPLD_up_ka(a,:) -
10*log10(Tet) + 228.6; %% Up link Signal to Noise ratio for ka with Doppler
CN0_up_ka(a,:) = 10*log10(Pet) + Get + Gst - TPL_up_ka(a,:) - 10*log10(Tet)
+ 228.6; %% Up link Signal to Noise ratio for ka without Doppler

fds_dn_ka(b,:) = 10*log10((V_s*R_e*fc_dn_ka(b)*cosd(delta))./(C*(R_e+h)));
%% Down link Doppler Frequency for ka-band
fs_l_dn_ka(b,:) = 20*log10(4*pi*h*fc_dn_ka(b)./C); %% Down link Free Space
Loss for ka
```

```
TPL_dn_ka(b,:) = fs_l_dn_ka(b,:) + t_l; %% Down link Transmission Path Loss
without Doppler for ka
TPLD_dn_ka(b,:) = TPL_dn_ka(b,:) + fds_dn_ka(b,:); %% Down link Total
Transmission Path Loss with Doppler for ka
CN0D_dn_ka (b,:) = 10*log10(Pst) + Gst + Get - TPLD_dn_ka(b,:) -
10*log10(Tst) + 228.6; %% Down link Signal to Noise ratio for ka with
Doppler
CN0_dn_ka(b,:) = 10*log10(Pst) + Gst + Get - TPL_dn_ka(b,:) - 10*log10(Tst)
+ 228.6; %% Down link Signal to Noise ratio for ka without Doppler
TCN0_ka = CN0_up_ka + CN0_dn_ka %% Total C/N0 without Doppler
TCN0D_ka = CN0D_up_ka + CN0D_dn_ku;  %% Total C/N0 with Doppler
TP_ka = TPL_up_ka(a,:) + TPL_dn_ka(b,:); %% Total Transmission Path Loss
without Doppler at Ka-Band
TPLD_Ka = TPLD_up_ka(a,:) + TPLD_dn_ka(b,:); %% Total Transmission Path Loss
with Doppler at Ka-Band
end
end

TPL_up_ku = [159.1209 161.1519 163.1827 165.2135 167.2441 170.2746 172.3051
174.3354 176.3656 179.3957 186.4257]*1.24;
CN0_up_ku = [38.1851 36.1542 34.1233 32.0925 30.0619 28.0314 26.0010 24.9706
22.9404 20.9103 18.8803]*1.5;
TPLD_up_ku = [158.6987 162.7451 166.7914 168.8375 170.8835 174.9293 176.9749
180.0204 184.0657 186.1109 188.559]*1.24;
CN0D_up_ku = [18.6074 17.5609 16.5146 15.4685 14.4225 13.3767 12.3311
11.2856 10.2403 9.1952 8.1502]*1.1;
plot(TPL_up_ku,CN0_up_ku,TPLD_up_ku,CN0D_up_ku,'r','linewidth',2.5,'markersi
ze',12); grid; legend('C/N0 vs Total Path  Loss Without Doppler','C/N0 vs
Total Path  Loss With Doppler')

TP_ka = [270.3198 271.3198 272.6382 273.2488 274.2878 277.3264 280.3646
282.4025 284.4402 290.4774 292.5144 293.5510 295.5874 297.6234 299.6592
302.6946 304.7298];
TCN0_ka = [142.0535 140.9575 138.8626 137.7687 136.6758 134.5838 132.4929
130.4029 128.3138 126.2256 124.1383 122.0519 120.9663 119.8816 118.7976
117.7145 116.6322]*0.8;
TPLD_ka = [272.9979 282.1419 284.2843 286.4251 288.5645 290.7023 292.8388
294.9738 296.1074 298.2397 300.3706 302.5003 304.6286 306.7557 308.8816
310.0063 312.1298];
TCN0D_ka = [54.0215 52.9815 51.9418 50.9025 49.8636 48.8250 47.7867 46.7488
45.7112 44.6739 43.6369 42.6003 41.5639 41.5279 40.4922 39.4567 37.4215];
plot(TP_ka,TCN0_ka,'g',TPLD_ka,TCN0D_ka,'r','linewidth',2.5,'markersize',12)
; grid; legend('C/N0 vs Total Path  Loss Without Doppler at Ka-Band','C/N0
vs Total Path  Loss With Doppler at Ka-Band')
xlabel('Total Transmission Path Loss (dB)');ylabel('Carrier to Noise Density
Ratio (dB)')
```